



RESEARCH PAPER

Development of a sink–source interaction model for the growth of short-rotation coppice willow and *in silico* exploration of genotype×environment effects

M. Cerasuolo^{1,*}, G. M. Richter^{1,†}, B. Richard¹, J. Cunniff², S. Girbau², I. Shield², S Purdy³ and A. Karp²

¹ Sustainable Soils and Grassland Systems Department, Rothamsted Research, Harpenden, Herts AL5 2JQ, UK

² Agroecology Department, Rothamsted Research, Harpenden, Herts AL5 2JQ, UK

³ Institute of Biological Environmental and Rural Sciences (IBERS), Aberystwyth University, Plas Gogerddan, Aberystwyth, Ceredigion SY23 3EE, UK

* Present address: Department of Mathematics, University of Portsmouth, Lion Gate Building, Lion Terrace, Portsmouth, Hampshire PO1 3HF, UK.

† To whom correspondence should be addressed. Email: goetz.richter@rothamsted.ac.uk

Received 29 August 2015; Revised 5 November 2015; Accepted 6 November 2015

Editor: Elizabeth Ainsworth, USDA/ARS

Abstract

Identifying key performance traits is essential for elucidating crop growth processes and breeding. In *Salix* spp., genotypic diversity is being exploited to tailor new varieties to overcome environmental yield constraints. Process-based models can assist these efforts by identifying key parameters of yield formation for different genotype×environment (G×E) combinations. Here, four commercial willow varieties grown in contrasting environments (west and south-east UK) were intensively sampled for growth traits over two 2-year rotations. A sink–source interaction model was developed to parameterize the balance of source (carbon capture/mobilization) and sink formation (morphogenesis, carbon allocation) during growth. Global sensitivity analysis consistently identified day length for the onset of stem elongation as most important factor for yield formation, followed by various ‘sink>source’ controlling parameters. In coastal climates, the chilling control of budburst ranked higher compared with the more eastern climate. Sensitivity to drought, including canopy size and rooting depth, was potentially growth limiting in the south-east and west of the UK. Potential yields increased from the first to the second rotation, but less so for broad- than for narrow-leaved varieties (20 and 47%, respectively), which had established less well initially (–19%). The establishment was confounded by drought during the first rotation, affecting broad- more than narrow-leaved canopy phenotypes (–29%). The analysis emphasized quantum efficiency at low light intensity as key to assimilation; however, on average, sink parameters were more important than source parameters. The G×E pairings described with this new process model will help to identify parameters of sink–source control for future willow breeding.

Key words: Carbon allocation, genotype, modelling, *Salix*, sensitivity analysis, sink–source interaction.

Introduction

Yield improvement is an important objective in the development of woody biomass feedstocks from short-rotation coppice (SRC) (Volk *et al.*, 2006; Karp and Shield, 2008). Poplar

(*Populus* spp.) and willow (*Salix* spp.) are comparatively young in their domestication (Karp *et al.*, 2011; Stanton *et al.*, 2014) and pedo-climatic adaptation (Aylott *et al.*, 2008;

Toillon *et al.*, 2013). However, yields have been doubled by breeders selecting mainly for total harvestable biomass, stem traits, and disease resistance (Karp *et al.*, 2011). Traits associated with vigour (Kauter *et al.*, 2003; Weih and Nordh, 2005; Volk *et al.*, 2006; Verlinden *et al.*, 2013), development (Verwijst *et al.*, 2012; Toillon *et al.*, 2013), photosynthesis (Robinson *et al.*, 2004; Andralojc *et al.*, 2014), and water-use efficiency (Weih and Nordh, 2002; Deckmyn *et al.*, 2004) are now also being incorporated. However, experimental evidence for carbon assimilation (source formation) and its linkage to allocation (sink formation) to above-ground biomass (AGB) (Bullard *et al.*, 2002b; Laureysens *et al.*, 2003; Guidi *et al.*, 2009) and below-ground biomass (BGB) (Heilman *et al.*, 1994; Matthews, 2001; Rytter, 2001; Martin and Stephens, 2006; Pacaldo *et al.*, 2013) has yet to be integrated.

Process-based simulation models are useful tools for integrating knowledge and assessing the relative importance of traits, particularly in woody perennials with long growth cycles, where gathering experimental data is time consuming and expensive (Karp *et al.*, 2014). SRC comprises successive harvest (coppicing) rotations lasting 2–3 years, where ‘regrowth’ after harvest occurs from basal buds on coppiced stools, while successive ‘annual growth’ before harvest occurs from buds on the stems. Annual regrowth from reserves was poorly addressed in early models (Le Roux *et al.*, 2001), despite its importance (Ceulemans *et al.*, 1996; Philippot, 1996). The existing models for SRC treat growth either as source dependent (‘top down’), limited by light interception and use efficiency (Tharakan *et al.*, 2008), or as sink dependent (‘bottom up’) and influenced by coppice response and carbon allocation (Deckmyn *et al.*, 2004). For phenological development, a simple empirical canopy model (Deckmyn *et al.*, 2004) was later replaced by a temperature-controlled budburst model (Deckmyn *et al.*, 2008), and adapted for SRC without validation (Tallis *et al.*, 2013). The need to model temperature control of dormancy, currently debated in many species (Fu *et al.*, 2012), is also unclear in willow (Savage and Cavender-Bares, 2011). Indeed, the whole system of yield formation, dormancy break, budburst, and start of photosynthesis needs to be integrated with the initiation of stem growth (sink formation).

Carbon allocation and sink formation have often been simplified in previous models (Deckmyn *et al.*, 2004) and allocation to BGB reserves ignored, despite its potential importance for regrowth after coppicing (Tschaplinski and Blake, 1995; Ceulemans *et al.*, 1996). Control of early soft-wood production by labile carbon allocated to tree reserves (Deckmyn *et al.*, 2008) has recently been observed for SRC (Verwijst *et al.*, 2012). The importance of reserves for regrowth was also shown in perennial forage crops (Schapendonk *et al.*, 1998; Teixeira *et al.*, 2007). For grassland, a sink–source interaction model was proposed (Schapendonk *et al.*, 1998) where assimilate allocation is controlled by sink formation. A similar control has been implemented for carbon partitioning in forest models (Fourcaud *et al.*, 2008; Pretzsch *et al.*, 2008). Carbon translocation is important for both SRC and grass, which show die-back of stems and tillers, respectively. Data from empirical protocols (stem number, length, and diameter), used for SRC phenotyping, can be used for the development of a hybrid model, which combines morphometric data with

an eco-physiological process model as suggested by Pretzsch *et al.* (2008). This is similar to the approach to predict yields of specific willow clones proposed by Amichev *et al.* (2011).

To simulate growth processes sufficiently well for use in willow breeding, there is a clear need to derive an integrated model that adequately incorporates key phenological processes and morphogenesis controlling AGB, while also taking into account BGB and the influence of reserves. In particular, it is important to integrate new experimental evidence, assess sink and source limitations, rank genotype-specific parameters, and identify the most important ones to focus breeding efforts.

To address these challenges, we developed a sink–source interaction model, LUCASS (light use and carbon allocation in *Salix* species) in which phenology controls growth and yield formation. This model describes and predicts the growth of four commercial willow genotypes. The model was calibrated for potential and water-limited production using detailed field data at two different sites in the UK. Key parameters for yield formation, across varieties and in different environments, were identified using a global sensitivity analysis (SA), including all parameters. Finally, the model was validated against independent growth and yield datasets.

Materials and methods

Field experiments

Detailed observations describing plant growth were recorded in two identical field trials laid out in a randomized block design consisting of four blocks (Cunniff *et al.*, 2015). Each block contained four commercial *Salix* varieties: Endurance (*Salix redheriana* × *Salix dasyclados*), Resolution (multiple parental crosses of *Salix viminalis* × *Salix schwerinii*), Terra Nova [*S. viminalis* × *Salix triandra*] × *Salix miyabeana*], and Tora [*S. schwerinii* × (*S. viminalis* × *S. viminalis*)] in individual plots of 224 m². Details can be found in Cunniff *et al.* (2015, see Table 1). These varieties were grouped according to growth and canopy phenology (see Supplementary Fig. S1 at *JXB* online) into broad-leaved (20–27 mm), closed canopy (Endurance, Terra Nova) and narrow-leaved (14–19 mm), open canopy (Resolution, Tora). The crops were planted in double rows (16 000 cuttings ha⁻¹) in May 2009 and coppiced in January 2010, 2012, and 2014. Destructive and non-destructive measurements of AGB and BGB traits were taken from respective plot areas during two successive 2-year rotations (R1, first rotation, 2010–2011; R2, second rotation, 2012–2013) to populate an extensive database for research and model development.

Locations

The experiments used for model parameterization (where previous data were not available), calibration, and internal evaluation were located in south-east England (51.82° N, 0.38° W) at Rothamsted (ROTH) and Aberystwyth (ABER) in Wales (52.4139° N, 4.014° W). Soils were characterized as a silty clay loam (chromic Luvisol; 1 m depth) and a shallow sandy silt loam (eutric endoleptic Cambisol; 0.55 m depth), respectively. Harvested yields were available for three of the four varieties, which were collected from successive 2- and 3-year rotations from separate trials at Long Ashton (LARS) in Somerset, England (51.43° N, 2.65° W) and ROTH between 2001 and 2010, were used for external model validation. LARS soil was classified as a coarse loam over clay (stagnogley) to clay (argillic Pelosol) (see Supplementary Table S1 at *JXB* online).

The long-term averages characterize ROTH as drier with a higher probability of water stress (WS) (704 mm, 9.3 °C) than ABER (1038 mm, 9.7 °C). Site-specific hourly weather data were recorded. The first rotation (R1, 2010–2011) was drier, while the second rotation (R2), especially 2012, was wetter than the long-term average (see Supplementary Fig. S2 and Supplementary Table S2 at *JXB* online).

Over all years, annual radiation at ROTH was about 20% higher and the temperature range (T_{\min}/T_{\max}) wider than at ABER (Table 1).

Phenotyping

Budburst was recorded annually (2010–2013), and buds were scored on 10 trees from early February twice weekly until bud swelling and then checked daily. Adapting a 7-point scale (Weih, 2009), budburst was defined as green leaf tips (<5 mm) being visible. Senescence was scored weekly from September to October using 10 trees per treatment and block, adapting a 7-point scale (Fracheboud *et al.*, 2009), defining its onset as >25% yellow/brown and <10% abscised leaves.

Plant architecture (height, stem length and diameter, and number of stems) was assessed on two pairs of trees, randomly chosen from the non-destructive area of each plot. Leaf area indices (LAIs) were estimated at ROTH twice monthly using the SunScan Canopy Analysis system (Delta-T Devices Ltd, Cambridge, UK); for details see Cerasuolo *et al.* (2013). Light-use efficiency (LUE) was estimated from simulated cumulative woody stem biomass and absorbed photosynthetic active radiation (APAR) based on calibrated LAIs.

Carbon allocation rates to AGB and BGB components were determined during the first rotation (2010–2012) by destructively sampling two complete trees per plot at key phenological stages

Table 1. Meteorological indicators during dormancy (November–March) and growth (April–October) periods

Mean maximal and minimal air temperatures (T_{\max} and T_{\min} , respectively) and cumulative annual global radiation (R_g) and precipitation (P) were recorded at the three sites.

Site	Dormancy		Growth		R_g (MJ m ⁻²)	P (mm)
	T_{\max} (°C)	T_{\min} (°C)	T_{\max} (°C)	T_{\min} (°C)		
ROTH	7.6	1.8	17.7	9.0	3910	680
ABER	9.0	3.8	16.6	11.6	3560	1020
LARS	9.2	3.1	18.5	10.4	3740	760

(Cunniff *et al.*, 2015). Stool (including remnant cut stem) and roots were excavated to a depth of 0.3 m, which is likely to represent >90% of the BGB (Pacaldo *et al.*, 2013). Destructive measurements of leaf weight and area were recorded (Cerasuolo *et al.*, 2013). During the second rotation (2012–2013), the number of destructive samples was reduced to twice a year, and final yields were assessed after each 2-year coppicing cycle (Cunniff *et al.*, 2015).

Model description

The process-based willow growth model LUCASS (Fig. 1) simulates development and growth of *Salix* spp. at the stand scale, considering phenological (budburst, growth, senescence, and dormancy) and morphological plant development (sink formation), and light interception, photosynthesis, and respiration (source formation). The AGB organs (leaves, branches, and stems) and BGB organs (stool and all roots) are considered as sinks, and the carbon allocation to these sinks is phenologically controlled and balanced within the sink–source interaction model (Schapendonk *et al.*, 1998). The sinks are phenologically dimensioned by stem and leaf numbers, their respective elongation rates, and specific dry matter densities, which define the carbon demand from a common source pool fuelled by photosynthesis and mobilizable reserves.

These processes are controlled by external variables (global radiation, air temperature, and water availability), provided by an environmental modelling framework (Richter *et al.*, 2006, 2010) that simulates the water and energy balance. LUCASS follows a bottom-up approach where light interception, photosynthesis, and respiration (Goudriaan and van Laar, 1994) are simulated with an hourly time step as part of the energy balance. Assimilate allocation to biomass components (leaf, branch, stem, stool, and roots) and respective reserve pools are calculated daily. Source–sink carbon flows are considered independently; however, carbon from senescing biomass (leaves, branch die-back, and fine roots) is translocated to the reserves.

Phenology

LUCASS simulates the multi-annual cycle of phenological development at the centre of process control (Fig. 1): budburst and leaf emergence, growth of individual organs, senescence and stem

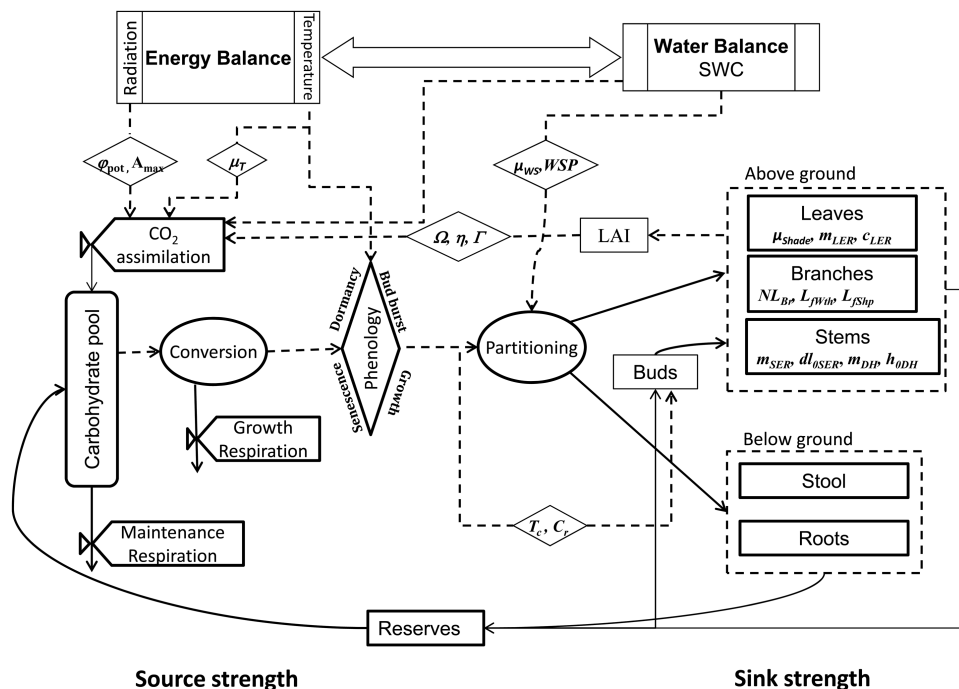


Fig. 1. Flowchart of the process-based willow growth model LUCASS, embedded into a water and energy balance framework. See text for details.

die-back, and dormancy to control the onset and duration of carbon capture (source formation) and its allocation to various sinks, as has been done in grape vine (Vivin *et al.*, 2002).

Budburst, leaf emergence, and elongation—Similar to earlier work (Tallis *et al.*, 2013), the budburst was simulated by combining a chilling phase followed by a forcing period (Chuine, 2000; Hlaszny *et al.*, 2012). Budburst dates were calculated (Eq. S1 at *JXB* online) using daily mean air temperature (T_{avr}), a half-efficiency temperature (T_C) and a chilling threshold (C_r); both T_C and C_r were estimated using genotype-specific budburst data. The other parameters defining the temperature response curves were adapted from Hlaszny *et al.* (2012). Chilling unit accumulation started with senescence during the previous season. In keeping with the known biology (Rinne *et al.*, 2011), negative chill units (C_w) accumulate during endodormancy until plants reach C_r (Cesaraccio *et al.*, 2004). At this point, the model plants enter ecodormancy, an inactive ‘standby’ phase, to accumulate daily forcing (anti-chill) units (C_a), which results in budburst when $C_r + \sum C_a \geq 0$.

Leaf emergence rate was calculated as suggested by Porter *et al.* (1993) and adjusted by photoperiod, water availability, and level of reserves (Eq. S2 at *JXB* online). The leaf emergence declined exponentially over the year. The potential leaf elongation rate was considered to be dependent on average temperature and day length (McDonald and Stadenberg, 1993), modified for plant age (Robinson *et al.*, 2004) and WS (Eq. S3 at *JXB* online).

Senescence and canopy duration—The model considers leaf senescence as a function of age (accumulated thermal time, μ_T), shading (μ_{shade} , LAI > 3), and WS (μ_{WS}). The start of senescence depends on a threshold day length, while the date of growth cessation (budset) is modelled as a function of accumulated thermal time; both values were estimated using experimental data (senescence score; end of stem extension) collected at ROTH and ABER during R1.

Stem and woody biomass development—Experimental evidence suggested modelling the onset and rate of stem extension as a function of day length (Eq. S5 at *JXB* online) with a developmental switch considering the base temperature for stem elongation ($T_{bstE} = 10^\circ\text{C}$). This is in contrast to grass models in which leaf and stem extension are determined by temperature (Schapendonk *et al.*, 1998; Hoeglin *et al.*, 2005). The dynamics of stem number is described by a function of the number of initial buds that form stems and their calibrated die-back rate. The demography of leaves (Porter *et al.*, 1993) and stems (Schapendonk *et al.*, 1998; Hoeglin *et al.*, 2005) was incorporated in order to consider the empirical evidence for regrowth after coppicing, e.g. die-back (self-thinning) of stems. The model does not consider plant mortality (Bullard *et al.*, 2002b) but rather plant density.

Sink formation

Leaf area and biomass—Total leaf area is a function of leaf number, size, and shape, scaled to LAI (Eq. S4 at *JXB* online). Initially, willow varieties produce a large number of small shoots in order to rapidly increase leaf area. These branches were treated as ‘super-leaves’ (long leaves whose area is equal to the cumulative area of leaves on the branch), whose growth rate follows the normal leaf emergence and elongation rate. The leaf area is converted to leaf biomass using a dynamic specific leaf area ($SLA_{min/max}$; Schapendonk *et al.*, 1998) that accounts for observed variable leaf weight and area ratios (Cunniff *et al.*, 2015), thickness, and variable level of reserves. In the model, mobilizable leaf carbon is translocated during senescence (e.g. leaves becoming lighter).

Stem and woody biomass—Potential stem elongation is modelled using a linear function of day length multiplied by a Heaviside function for the effect of daily average air temperature (Powers *et al.*, 2006) (Eq. S5 at *JXB* online).

The woody growth potential is expressed in terms of total dry biomass production, which was computed from the average stem

volume and specific stem dry weight, multiplied by the observed/simulated number of stems still alive. The stem volume depends on stem length and diameter/height ratio (m_{DH} ; Eq. S6 at *JXB* online) modified by a shape parameter η_{St} (Eq. S7 at *JXB* online), as stems are not exact cylinders.

Below-ground biomass—The stool and coarse and fine roots are the components of BGB modelled defining respective elongation rates, radial extension, and specific densities. Parameters of root extension and dry matter accumulation were calibrated against observed data (Cunniff *et al.*, 2015) on the basis of seasonal allocation (de Neergaard *et al.*, 2002) and respiration, as well as turnover (Rytter, 2001) rates of fine root dry matter.

Source formation

Light interception—The genotype-specific light interception is described by a pseudo-3D architectural model (Cerasuolo *et al.*, 2013), which defines horizontal and vertical spatial distribution of leaves in a gap fraction model, characterizing LAI distribution by clumping (Ω) and profile shape (η) factors. The LAI is computed daily and the cumulative LAI is considered as $\Omega \times L_c(z)$, where $L_c(z)$ is the distribution of leaf area over the canopy depth (z). The light interception module describes the effect of canopy clumping on both direct and diffuse radiation (De Pury and Farquhar, 1997). The extinction coefficient for the diffuse radiation is calculated according to Goudriaan (1988), with weighted contributions from the three zones of a standard overcast sky. To simulate light interception, the canopy is divided into five layers, which are either uniformly or asymmetrically distributed. Within each layer, the ratio of sunlit/shaded leaf area is calculated to estimate the vertical variation of photosynthesis inside the canopy.

Photosynthesis and carbon pools—Photosynthesis is computed as the assimilation rate of CO_2 using the maximum between an exponential function of the intercepted energy (APAR) and its potential absorption, modified by CO_2 air concentration and air temperature (Goudriaan and van Laar, 1994). The effect of soil water availability on stomatal conductance and reduction in CO_2 absorption is represented using a logistic function to describe the reduction of photosynthesis with decreasing relative soil water content (Sinclair, 1986).

Three different biochemical pools are simulated: first, a source pool of available carbohydrates (C_{av}) composed of photosynthetic assimilates and remobilized reserves used for growth and maintenance processes; secondly, a source–sink pool of mobilizable carbohydrate reserves (e.g. starch) in leaves, wood, and stool; and finally, the sink pool of structural biomass, divided into AGB (stems, branches, and leaves) and BGB (stool, and coarse and fine roots).

Sink–source interaction

Carbon allocation—The allocation of C_{av} is modelled as a combination of a sink–source balance and a hierarchical cascade [leaf > stem ≈ (pooled stool and coarse and fine roots)]. The respective sink strengths result from genetically determined growth potentials (see above) defined by the maximum rate of each organ’s dry matter accumulation and turnover (Genard *et al.*, 2008).

The total source (C_{av} ; Eq. 1a) to satisfy sink demands is calculated as the net daily integral of the difference between hourly leaf photosynthesis (CH_2O) and maintenance respiration of the respective tree organs (R_t ; Eq. 1b), plus the mobilizable reserves from leaves (Lf_{Res}), woody biomass (W_{Res}), and stool (Stl_{Res}):

$$C_{av} = CH_2O - R_t + Lf_{Res} + W_{Res} + \alpha \times Stl_{Res} \quad (1a)$$

$$R_t = (m_{Lf} \times Lf + m_B \times B + m_{Stl} \times Stl) \times Q_{1010}^{\frac{T_{avr} - T_{Q10}}{10}} \quad (1b)$$

A fraction of Stl_{Res} ($\alpha=0.04$) can be mobilized for 20 d after budburst (Deckmyn *et al.*, 2008; ANAFORE Manual). If new assimilates exceed sink demands (Schapendonk *et al.*, 1998), the emerging surplus of assimilates is allocated to the reserve pools. The available carbohydrates for AGB (AGB_{av}) are converted into leaf (LfB) and woody stem (WSB) biomass using their respective conversion factors (Penning de Vries *et al.*, 1983) and potential sink increases:

$$LfB = AGB_{av} \times LGrPt / ShGrPt, \quad (2a)$$

$$WSB = AGB_{av} \times SGrPt / ShGrPt. \quad (2b)$$

Here, $ShGrPt$ represents the total shoot growth potential, and $LGrPt$ and $SGrPt$ the leaf and stem growth potentials, respectively.

C_{av} is partitioned between AGB_{av} and BGB_{av} using constant potential allocation coefficients, derived from the experimental evidence. These allocation coefficients change with stool size to account for increasing plant vigour during establishment and drought to increase root growth for better resource capture (Goudriaan and van Laar, 1994).

$$StlB = BGB_{av} \times StlGrPt / BGGGrPt \quad (3a)$$

$$RtB = BGB_{av} \times RtGrPt / BGGGrPt \quad (3b)$$

Stool and roots are assumed to turn over with different rates; stools are set to have a longevity, which corresponds to the stand/plant lifetime (Bullard *et al.*, 2002b), while fine roots are set to a short mean residence time (0.25 years; Rytter, 2001).

Consecutively, C_{av} is allocated to the plant organs according to their respective sink strengths, defined by LAI and SLA, wood volume and density, stool mass, root growth, and turnover. Daily carbon allocation is, therefore, either limited by C_{av} , or by the effective sink demand of assimilates (potential growth). At each time step, LUCASS balances the gain and consumption of carbon, estimates the conversion of C_{av} into growth, and calculates the produced biomass for each component (g m^{-2} upscaled to kg ha^{-1}).

Effects of the environment—The soil hydrology is modelled using an energy balance approach combined with a two-layer soil water module (Richter *et al.*, 2006). The energy fluxes at the canopy surface are controlled by crop characteristics (LAI, stomatal resistance, canopy height), climatic variables, and soil hydraulic properties, e.g. water retention curves (see Supplementary Table S1 at *JXB* online), and resource capture (water uptake). The rooting depth is dynamic and is calculated using a constant crop-specific root advancement coefficient and maximum (plant \times soil) rooting depth. The soil water balance, transpiration, and water uptake are calculated using the Penman–Monteith equation. The plant WS variable, k_{WS} , is described by a non-linear, logistic function (Eq. S2c at *JXB* online) dependent on the relative water content between minimum and maximum plant-available soil water (Sinclair, 1986). Its curvature is determined by the WS parameter, WSP (Table 2), which was calibrated using the drought season (R1) data at ROTH. AGB/BGB partitioning is modified according to soil water availability (van Laar *et al.*, 1992).

The effects of WS on leaf emergence and elongation rates, and stem and leaf mortality are also considered as a function of k_{WS} and respective potential rates. Buds and branches follow the same dynamics as leaves, but the mortality rate of branches is assumed to be 10 times lower than that of leaves. The mortality rate of stems is also computed as the sum of natural turnover and death rate caused by water and shading stress; however, stem mortality is less than that of leaves ($\mu_{WS/T} 2 \times 10^{-4}$ and $1.2 \times 10^{-3} \text{ d}^{-1}$, respectively).

Calibration and parameter ranking

The model inputs divide into environmental variables and process parameters: (i) field location (longitude, latitude, etc.) and soil characteristics; (ii) management data (irrigation, harvest days, number

of years per growth cycle); (iii) (hourly) weather data, e.g. solar radiation, mean air temperature, wind speed and direction, rainfall and air humidity; and (iv) genotype-specific growth parameters.

Model calibration

The parameters of the growth model were calibrated using genotype-specific experimental data where values from the literature were not available (Table 2). Process-specific evidence was used to calibrate development and morphology either through direct measurements (e.g. leaf emergence and senescence) or through parameter estimation involving model data fitting (e.g. budburst, stem height, and stem diameter). Model cross-validation was performed using a time series of the variables not used for calibration (e.g. canopy height, stem biomass). The photosynthesis parameters (Bonneau, 2004) were calibrated to match total biomass production and turnover.

Parameters of the budburst model (Eq. S1 at *JXB* online) were calibrated using ROTH data from the first rotation cycle (R1, 2010–2011), while parameters for stem height/diameter relationships were estimated using data from both locations (ABER and ROTH, 2010–2011). LUCASS (remaining parameters) was calibrated for potential productivity using data from ABER assuming that water was unlikely to limit growth and carbon partitioning, especially in R2. The flux parameters for carbon allocation were calibrated using morphological components of AGB (leaf and stem weight) and BGB (stool and fine root weight). In a final step, the WS effect on biomass production was calibrated using a time series of data collected at ROTH in R1 (e.g. LAI).

Sensitivity analysis

A global SA was performed for all varieties and both sites for potential (no water stress, NWS) and actual (WS) growth, and the model response was determined for the first and second coppice rotations (R1 and R2). The aim was to understand which growth parameters had a significant impact on final yield, and whether it changed with the environment, age of stand or phenotype. All of the 78 parameters (Table 2) were varied in a one-at-a-time modus using the Morris method (Morris, 1991). Assuming that all parameters were normally distributed (Richter *et al.*, 2010), the window of their variation was set to a respective standard deviation of 10%. The estimated average response strength (μ) for each parameter represents its overall effect on the model outcome (e.g. final yield). Its standard deviation (σ) represents the response spread estimating higher-order effects (non-linearity, parameter interactions). Both μ and σ were calculated over six different trajectories (individual one-parameter-at-a-time simulations) and using six levels (granularity of the explored parameter space) (Richter *et al.*, 2010).

Data analysis and model validation

Data were analysed with Genstat™ 14 (Payne *et al.*, 2011) to examine the influence of location and varieties using a two-way ANOVA. Linear regressions were performed using Sigmaplot (version 12.0, 2011). The model was validated against yield data from the second growth cycle at ROTH, and independent datasets for three of the four varieties at LARS and ROTH. The goodness of simulations to match experimental data for the two dedicated trials was characterized with the residual mean square error (RMSE). The coefficient of determination, the model efficiency (ME), RMSE, bias [mean difference (MD)] and r^2 were calculated according to Smith *et al.* (1997).

Results

All results fell into a distinct pattern due to significantly different climatic conditions during the two rotations where R1 was distinctly drier than R2, which translated into high WS, especially in 2010, and low WS, especially in 2012. These conditions were exacerbated by site differences and reached almost potential NWS conditions in ABER during 2012, while ROTH had strong WS conditions during R1 growth.

Table 2. Alphabetical list according to process domain of model parameters used in LUCASS

Symbols, definition, and units as well as source (reference, experimental evidence) are given.

Symbol	Definition	Units	Reference/comments
Phenology			
C_r	Chilling requirement	d	Optimized
d_{ac}	Number of day necessary to the crop to reallocate resources	d	Optimized
dd_{fill}	GDD for max stem filling rate	°C d	Calibrated
dl_{0SER}	Stem elongation rate, intersect	d	Measured
dl_{BtoBr}	Base photoperiod of buds becoming branches	d d ⁻¹	Assumed
$dl_{maxBtoBr}$	Photoperiod for maximum rate of buds becoming branches	d d ⁻¹	Assumed
$NBuds_0$	Initial bud number	–	Measured
T_B	Base temperature for above-ground growth	°C	Perttu and Philippot (1996)
T_{BG}	Base temperature for below-ground growth	°C	Assumed
T_{bStE}	Base temperature for stem elongation	°C	Calibrated
T_c	half-efficiency temperature	°C	Optimized
$T_{optBtoBr}$	Optimum temperature for buds becoming branches	°C	Calibrated
Morphology: sink formation			
a_{Stl}	Linear coefficient in the stool elongation rate	mm d ⁻¹	Calibrated
$a_{Stl/H}$	Linear coefficient in the linear relationship of stem height–stool weight	m g ⁻¹	Calibrated
b_{Rt}	Root elongation rate	m d ⁻¹ °C ⁻¹	Calibrated
b_{Stl}	Constant coefficient in the stool elongation rate	mm d ⁻¹ °C ⁻¹	Calibrated
$b_{Stl/H}$	Constant coefficient in the linear relationship of stem height–stool weight	m	Calibrated
C_{BtoBr}	Maximum relative rate of buds producing branches	d ⁻¹	Calibrated
C_{LER}	Leaf extension, constant	m	Porter <i>et al.</i> (1993)
f_{fill}	Power for stem filling rate	–	Calibrated
$ff_{maxBtoBr}$	Maximum proportion of buds that produce new branches	–	Calibrated
h_{0DH}	Relationship diameter/height intersect	mm	Measured
LAI_{CShade}	Minimum LAI for shading to cause senescence	m ² m ⁻²	Calibrated
I_{distr}	Leaf layers distribution	–	Cerasuolo <i>et al.</i> (2013)
L_{Shp}	Leaf shape factor	–	Measured
L_{Wth}	Leaf width	m	Measured
l_{SBr}	Relative reduction of branching with increased LAI	–	Calibrated
m_{DH}	Relationship of diameter/height slope	mm m ⁻¹	Measured
m_{LER}	Leaf elongation linear coefficient	m d ⁻¹	Porter <i>et al.</i> (1993)
m_{SER}	Stem elongation rate, slope	m d ⁻¹	Measured
NL_{Br}	Number of leaves per branch	–	Calibrated
n_{Stwt}	Power coefficient for the estimation of the stool weight factor	–	Calibrated
$n_{maxStlwt}$	Stool weight at which the stool weight factor reaches its maximum effect	g m ⁻²	Calibrated
ρ_{AG}	Fraction of assimilates going to the above-ground organs	–	Measured
ρ_{Rt}	Fraction of below-ground assimilates going to roots	–	Measured
ρ_{St}	Specific stem weight	g m ⁻²	Measured
SLA_{max}	Maximum specific leaf area	m ² g ⁻¹	Measured
SLA_{min}	Minimum specific leaf area	m ² g ⁻¹	Measured
St_{max}^t	Max stem number given the initial number of buds	–	Calibrated
η_{St}	Stems shape parameter	–	Assumed
μ_{Br}	Porter mortality factor—lower asymptote	–	Porter <i>et al.</i> (1993)
μ_W	Branches and stems aging death rate	d ⁻¹	Measured
μ_{WRes}	Percentage of woody reserves lost during the harvest	g g ⁻¹	Calibrated
σ_{Rt}	Root dry matter per unit length	g m ⁻¹	Calibrated
σ_{Stl}	Stool structural dry matter per unit length	g m ⁻¹	Calibrated
W_{loss}	Percentage of dry matter lost during the harvest	–	Calibrated
Physiology: source formation			
Light interception			
α	ELADP quadratic coefficient	–	Observed
β	ELADP linear coefficient	–	Observed
γ	ELADP constant	–	Observed
η	Shape parameter for the vertical leaf area distribution	–	Cerasuolo <i>et al.</i> (2013)
Ω	Clumping index	–	Cerasuolo <i>et al.</i> (2013)
μ_T	Temperature-driven increase of senescence	d ⁻¹	
$\mu_{maxShade}$	Maximum shading-induced senescence rate	d ⁻¹	Calibrated

Table 2. Continued

Symbol	Definition	Units	Reference/comments
μ_{Shade}	Shading-induced increase of senescence rate per unit of LAI	d^{-1}	Calibrated
μ_{WS}	Water stress-driven increase of senescence	d^{-1}	Calibrated
Assimilation and respiration			
A_{max}	CO_2 potential assimilation rate at light saturation	$\text{g}(\text{CO}_2) \text{m}^{-2} \text{s}^{-1}$	Bonneau (2004)
P_{cmax}	Max photosynthetic rate capacity	$\mu\text{g}(\text{CO}_2) \text{m}^{-2} \text{s}^{-1}$	Bonneau (2004)
ρ_{Lf}	Percentage of single leaves produced by new flushing buds	–	Calibrated
Q_{10}	Responsiveness of respiration at a temperature of 10 °C	–	Sampson and Ceulemans (2000)
r_b	Boundary layer resistance	s m^{-1}	Calibrated
R_{BG}	Maintenance respiration rate of roots	$\text{g}(\text{glucose}) \text{d}^{-1}$	Vivin et al. (2002)
R_{D}	Dark respiration	$\mu\text{g}(\text{CO}_2) \text{m}^{-2} \text{s}^{-1}$	Kaipainen (2009)
RES_{max}	Maximum reserve fraction	–	Calibrated
RES_{maxStt}	Maximum reserve fraction of stool dry matter	–	Calibrated
R_{Lf}	Maintenance respiration rate of leaves	$\text{g}(\text{glucose}) \text{d}^{-1}$	Vivin et al. (2002)
$r_{\text{s,min}}$	Minimum stomatal resistance	s m^{-1}	Bonneau (2004)
R_{St}	Maintenance respiration rate of stems	$\text{g}(\text{glucose}) \text{d}^{-1}$	Vivin et al. (2002)
T_{bC}	Base temperature in CO_2 assimilation	°C	Assumed
T_{maxC}	Maximum temperature in CO_2 assimilation	°C	van Laar et al. (1992)
T_{minC}	Minimum temperature in CO_2 assimilation	°C	
T_{optC}	Optimal temperature in CO_2 assimilation	°C	
WSP	Water stress parameter	–	Calibrated
Γ	CO_2 compensation point at 25 °C	$\mu\text{mol mol}^{-1}$	Xu et al. (2008)
ξ_{GW}	Conversion of assimilates to biomass	$\text{g}(\text{glucose}) \text{g}^{-1}$	Penning de Vries et al. (1983)
φ_{pot}	Quantum efficiency of photosynthesis	$\mu\text{g CO}_2 \text{J}^{-1}$	Bonneau (2004)
σ	Scattering coefficient of leaves for PAR	–	Goudriaan (1988)

Sensitivity Analysis

Identification and ranking of key parameters

The heat map details (see [Supplementary Fig. S3](#) at *JXB* online) showed a clear pattern of high sensitivity under potential (NWS) and low WS (R2) growing conditions, which translated clearly into the aggregated averages ([Fig. 2](#)). Considering a model response threshold of about 1000 kg ha^{-1} per 10% parameter change (4–5% yield potential), the SA revealed that yields were affected by up to 20 parameters (under NWS). Under conditions of growth-limiting WS, the number of parameters with significant effects on yield dropped to fewer than 10. However, these ranked consistently high when considering the average response to their variation across sites (ABER, ROTH), age (R1, R2), and canopy phenotype. Model sensitivity was higher in the second (R2) than in the first (R1) rotation ([Fig. 3](#)), most likely due to lower WS. Differences between sites were small overall and affected only a few parameters [day length associated with buds turning into branches (dl_{BtoBr}); AGB/BGB partitioning (ρ_{AB}), and quantum efficiency (φ_{pot})]. Most of these parameters reflected experimental evidence and measurable crop traits defining sinks and sources.

Sink formation: phenomorphology

The onset of stem elongation (dl_{SER}) was identified as the overall most important yield determining (phenological) parameters at both sites and for all conditions. It was followed by closely related morphological sink determinants, such as stem elongation rate (m_{SER}) and diameter/height coefficient (m_{DH}). The fraction of total biomass allocated to AGB

(ρ_{AG}) also ranked among the strongest effects, emphasizing the importance of AGB/BGB partitioning. The fraction allocated to roots (ρ_{R}) had an equally large effect ($0.7\text{--}2.3 \text{ Mg ha}^{-1}$). These sink parameters had the most stable ranking across most of the subsets of the SA; exceptions were rank changes for ρ_{AG} with site and phenotype.

Phenological parameters that determine budburst [chilling requirement (C_t); base temperature (T_c)] showed a very inconsistent and contrasting behaviour. C_t ranked higher overall for potential than water-limited growth, which was also reflected in its higher rank in the wet second rotation. Differences between sites were marginal, but both parameters were slightly more important for ABER than for ROTH (see [Supplementary Table S4](#) at *JXB* online); however, C_t ranked on average slightly higher for the open canopy phenotype ([Fig. 2](#)).

Source formation

Source-related parameters (light interception, photosynthesis) were on average less sensitive than sink-related parameters. Parameters of canopy structure (Ω ; η) were identified as important under potential (2.3 and 1.6 Mg ha^{-1}) but not under water-limited production ($<0.5 \text{ Mg ha}^{-1}$). On the other hand, parameters determining light interception, e.g. the number of leaves and leaf elongation rate ($>2 \text{ Mg ha}^{-1}$) ranked consistently high, irrespective of the site, rotation, or phenotype. The sensitivity of photosynthesis, quantum efficiency (φ_{pot}), was on average more than twice that of the CO_2 potential assimilation rate at light saturation (A_{max}), emphasizing light conversion at low light levels to be crucial for willow production in the UK. There was a difference between sites (see below)

		Average Strength								Rank of strength									
		All WS&NWS	All NWS	All WS	WS R1	WS R2	ABER WS R1+R2	ROTH WS R1+R2	WS END & TN	WS RES & T	All WS&NWS	All NWS	All WS	WS R1	WS R2	ABER WS R1+R2	ROTH WS R1+R2	WS END & TN	WS RES & T
Phenology	C_r	1535	2451	619	352	886	476	762	782	989	10	9	17	9	19	17	16	21	15
	dl_{BtoBr}	1866	2967	765	276	1254	355	1176	1344	1165	8	6	13	12	13	22	5	13	12
	dl_{BMax}	1161	1569	753	104	1402	497	1009	1832	973	15	16	14	24	10	15	10	7	16
	dl_{OSER}	9184	12083	6285	2441	10129	6641	5929	11941	8317	1	1	1	1	1	1	1	1	1
	f_{fill}	548	876	219	88	351	105	334	449	252	22	20	25	25	25	29	23	24	26
	dd_{fill}	420	539	301	146	456	205	396	588	324	24	22	23	21	23	24	22	23	24
	b_{Rt}	391	0	783	12	1554	765	801	1546	1561	25	34	11	32	9	11	15	11	7
	T_c	686	737	636	173	1098	435	836	1136	1060	20	21	16	19	16	20	14	15	13
Morphology	ρ_{AG}	2482	4147	816	302	1330	595	1037	1857	803	4	3	10	11	11	13	9	6	18
	h_{ODH}	504	479	529	272	786	451	607	787	785	23	24	20	13	21	18	18	20	19
	c_{LER}	986	1390	581	257	905	570	593	816	995	16	17	19	15	18	14	19	19	14
	m_{LER}	2011	2669	1354	718	1990	1523	1185	2061	1920	6	8	4	5	4	4	4	5	4
	m_{SER}	2978	4011	1945	998	2892	1791	2099	3502	2281	2	4	2	3	2	2	3	2	3
	m_{DH}	1781	2380	1182	751	1614	1248	1117	1788	1439	9	10	6	4	7	6	7	10	8
	NL_{Br}	2422	3601	1242	498	1986	1331	1153	2062	1910	5	5	5	7	5	5	6	4	5
	$NBuds_0$	658	986	330	257	404	397	264	388	420	21	19	22	16	24	21	25	25	22
	p_{Lj}	1381	1760	1001	234	1768	1126	876	1790	1746	12	14	7	18	6	7	13	9	6
	ρ_{Rt}	1425	1900	949	614	1285	946	953	1206	1364	11	12	9	6	12	8	11	14	10
	ff_{max}	844	1089	598	267	930	685	511	1095	765	18	18	18	14	17	12	21	16	21
	Light Interception	k_c	45	69	21	8	34	23	19	45	23	34	31	33	33	33	33	33	33
Ω		1301	2348	254	32	476	177	331	701	250	13	11	24	28	22	26	24	22	27
LAI_{cShade}		173	345	1	0	2	1	0	3	0	30	25	35	35	35	35	35	35	35
SLA_{max}		228	336	121	84	159	119	124	203	115	28	26	28	26	30	28	28	28	29
SLA_{min}		39	50	29	18	39	31	26	46	31	35	32	32	31	32	31	32	32	32
η		835	1577	94	22	166	71	117	265	68	19	15	30	29	29	30	29	26	30
Physiology		ρ_{20}	208	223	193	110	277	225	162	176	378	29	27	26	23	26	23	27	30
	φ_{pot}	2683	4655	710	254	1166	491	930	1465	867	3	2	15	17	14	16	12	12	17
	A_{max}	1189	1866	512	168	856	444	580	941	772	14	13	21	20	20	19	20	18	20
	μ_T	1938	2902	974	342	1607	869	1080	1813	1401	7	7	8	10	8	9	8	8	9
	μ_{Shade}	50	98	2	0	4	3	1	8	0	33	30	34	34	34	34	34	34	34
	μ_{WS}	384	0	767	431	1103	792	743	1001	1206	26	33	12	8	15	10	17	17	11
	$d_{AfterCut}$	363	537	189	144	233	202	175	210	256	27	23	27	22	27	25	26	27	25
	RES_{max}	157	196	118	35	200	139	96	191	210	31	28	29	27	28	27	30	29	28
	μ_w	96	159	34	20	48	25	43	63	33	32	29	31	30	31	32	31	31	31
	WSP	972	0	1944	1128	2760	1706	2182	2400	3120	17	34	3	2	3	3	2	3	2

Fig. 2. Heat map for the average of response strength (μ) estimated using the Morris method and ranking calculated for all varieties together or separated according to potential and water-limited conditions (all WS and NWS, all NWS, and all WS). Average sensitivity was calculated under water-limited conditions for the first (WS R1) and second (WS R2) rotations separately, for sites considering both rotations (ABER WS R1+R2 and ROTH WS R1+R2), and across similar canopy phenotypes (END & TN, Endurance and Terra Nova; RES & T, Resolution and Torá). Colour intensity increases with increasing response strength but is lower for higher ranks.

and phenotypes; the change of φ_{pot} was more important in large, closed-canopy phenotypes (END and TN).

Environmental effects

The overall parameter effects on yield were only marginally higher at ROTH than at ABER (0.73 and 0.81 Mg ha⁻¹; Fig. 3), but model sensitivity was higher in R2 than in R1, which reflected the wetter growth conditions in R2, while R1 was characterized by WS aggravated by higher cumulative radiation (Table 1). The relative sensitivity to changes of physiological parameters (photosynthesis) was similar for both sites when tested for potential production (NWS; Supplementary Table S4 at JXB online). The effects of WS reduced the overall

sensitivity to changes of other physiological parameters (light interception and photosynthesis).

The SA revealed interactions between process and site, e.g. resulting in different parameter rankings related to temperature [budburst and senescence (μ_T)] and water, both marginally more important at ROTH than at ABER. The high ranking of WSP did not translate into similar differences caused by variation of WS-induced senescence (μ_{WS}) (Fig. 2). At ROTH, the average effect of source-related parameters on yield, such as light interception (onset of branching, dl_{BtoBr} , number of leaves per branch, NL_{Br} , Ω , and η) and photosynthesis (φ and A_{max}) ranked lower than at ABER, which could reflect an interaction of light (lower radiation) and water

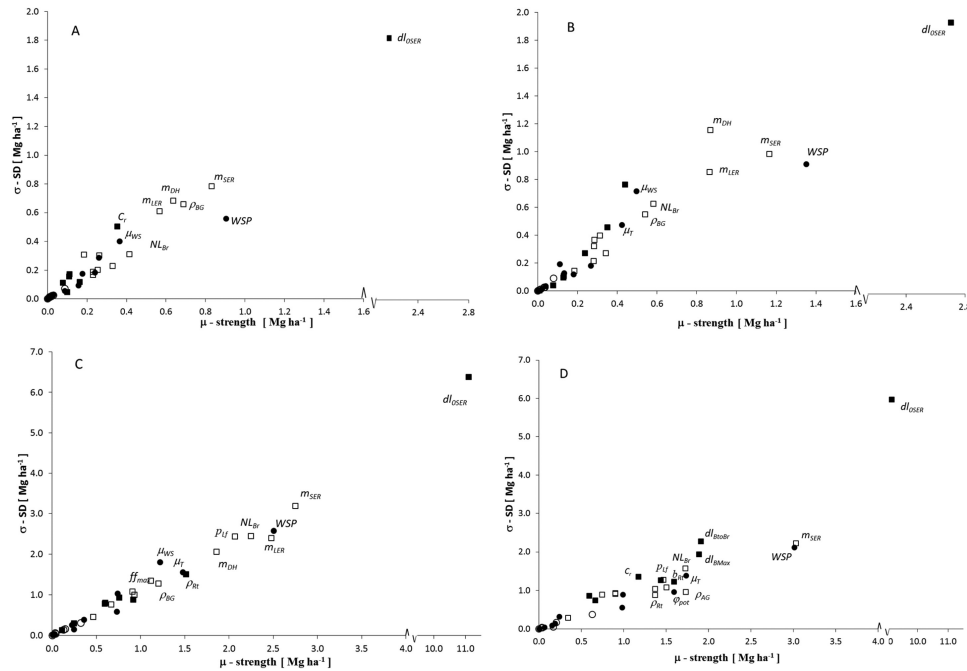


Fig. 3. Morris sensitivity measures (μ^* , σ) under water-limited production to random changes of 34 model parameters averaged across all genotypes for ROTH (A, C) and ABER (B, D) during the first and second rotations, respectively. Symbols represent phenological (closed squares) and morphological (open squares) sink-related parameters, and physiological (closed circles) and other source-related parameters (open circles).

availability. In contrast, parameters related to carbon allocation (sink size) ranked higher at ROTH than at ABER.

Model calibration and cross-validation

Phenology, light interception, and LUE

Budburst parameter values showed a small variation among varieties (see [Supplementary Table S3](#) at *JXB* online) with an average value of 6.1 ± 0.5 °C and -18.1 ± 0.4 for T_C and C_T , respectively. The model explained an overall 79% of the variance in budburst date at ABER. In 2013, budburst showed a reduced goodness of fit by more than 10% at both sites as temperatures were outside the range of calibration.

Light interception is the result of a complex process of leaf area formation (Eq. S2–S4 at *JXB* online). Leaf area was first calibrated at ABER using only destructive LAI measurements, and then recalibrated for WS against the experimental evidence of LAI at ROTH during the first rotation ([Fig. 4A, F](#)).

The LAI simulation at ROTH (Endurance and Tora in [Fig. 4A, F](#) and Resolution and Terra Nova in [Supplementary Fig. S4](#) at *JXB* online) was better during the first rotation than during the second (respective RMSE values for Endurance were 0.95 and 1.78, [Table 3](#)). This was mainly due to delayed canopy development after coppicing in January 2012. Overall, the model reflected the genotypic differences between canopy types quite well, but described LAI better for non-coppiced than for coppiced years (RMSE values of 0.76 and 1.26, respectively).

The parameters for photosynthesis were estimated against total biomass (e.g. [Fig. 4D, E](#), fine roots), and A_{\max} in the range of 18.9 – 23.3 $\mu\text{mol m}^{-2} \text{s}^{-1}$ matched the sink demand well. For Terra Nova, we calibrated a value similar to Endurance as both had a similar canopy. For

comparison, photosynthesis was also expressed in terms of LUE, based on annual woody AGB (stem yield) and simulated intercepted PAR ([Fig. 5A](#)) and averaged over all years ([Fig. 5B](#)). LUE was 6% lower during R1 compared with R2 at ROTH but not at ABER. LUE actually showed a site \times year \times phenotype effect. While LUE for narrow-leaved Tora recovered during 2011, it remained low for broad-leaved Endurance at ROTH due to drought. This was reflected in the respective yield drops in comparison with the R2 validation data (see below, 13 and 28%; see [Fig. 7](#)). At ABER, there were similar LUE increases for both phenotypes during 2011, which compensated for the overall low initial efficiency (2010), although not so at ROTH.

Sink formation: carbon allocation

Potential stem elongation rates were initially calibrated using stem height data during 2012 at ABER to avoid bias due to carbohydrate limitations and WS. The parameter values for stem elongation (Eq. S5 at *JXB* online) were then optimized through iteration using ABER genotype-specific growth data (time series) during the first rotation (2010–2011). These parameters fitted well with the heights observed at ROTH ([Table 3](#)). The agreement between computed and observed stem extension rates was reflected in the stem growth dynamics at ROTH, in particular for the variety Tora ([Fig. 4G](#)).

Stem number was strongly affected by the environment, with numbers significantly smaller at ABER than at ROTH ($P < 0.01$) during 2010–2011, and by genotype ($P < 0.001$) with Endurance having the most and Resolution the fewest. A significant interaction between sites and varieties ($P < 0.01$) was related to greater range in stem numbers among varieties at ROTH compared with ABER.

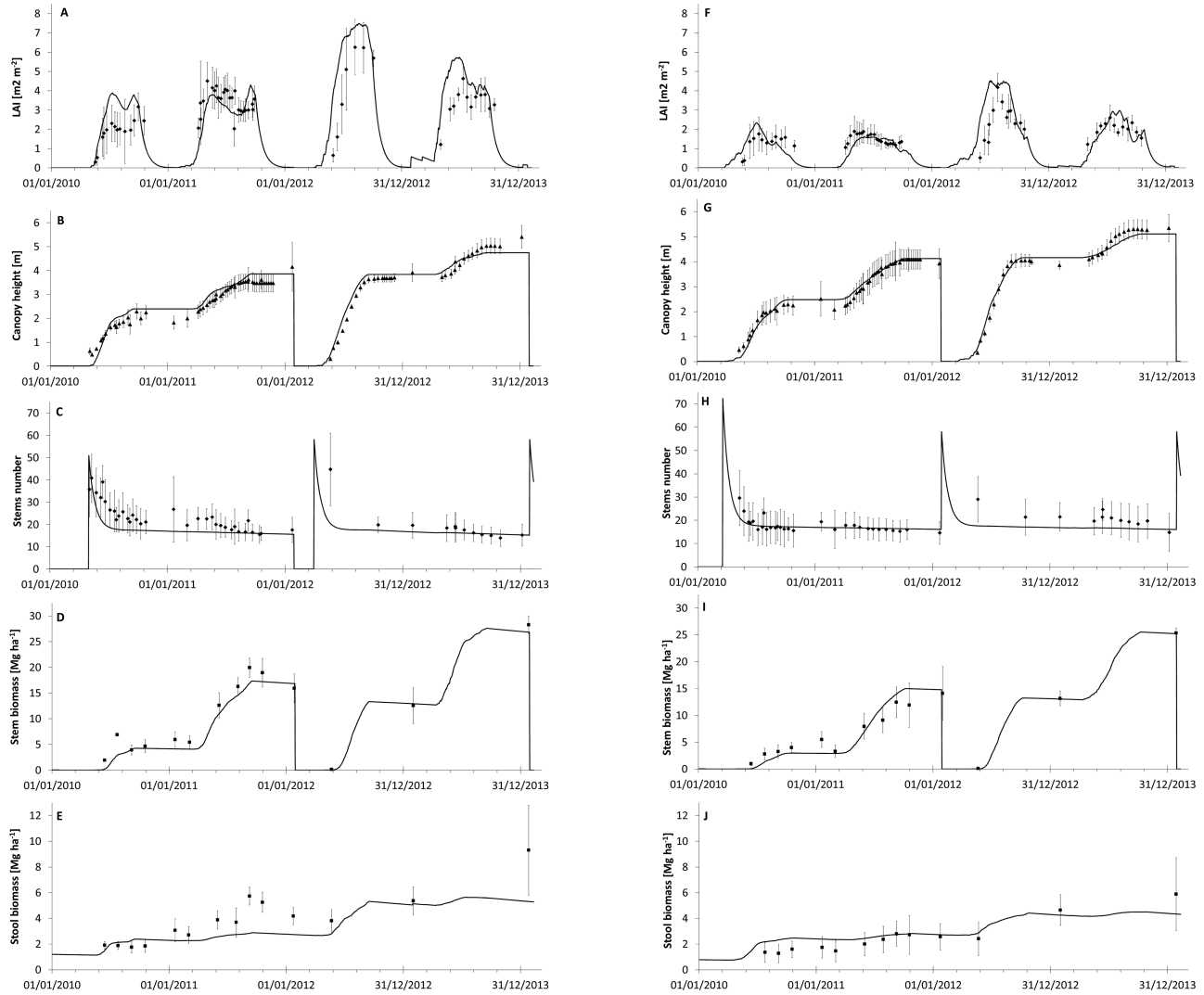


Fig. 4. Observed (filled symbols) and simulated (solid line) LAI, canopy height, stem number, and accumulated stem (AGB) and stool (BGB) yield of Endurance (A–E) and Tora (F–J) grown at ROTH over two consecutive rotations (2010–2011 and 2012–2013). The error bars represent the standard deviations of the experimental values ($n=4$).

The relationship between stem height and diameter also showed a strong interaction between sites and varieties (Fig. 6; $P<0.001$). The data showed two separate groups, one for ROTH where stems were thinner and the other for ABER where stems were thicker, for an equivalent height. The parameters m_{DH} and c_{DH} were evaluated for each variety at each site from the first rotation data (see Supplementary Table S5 at *JXB* online). These observations suggested a combination of site-specific parameter values for AGB/BGB partitioning and initial stem numbers and height/thickness (m_{DH}).

Destructive harvest data from both sites (R1) were used to approximate the partitioning between AGB and BGB (including coarse but not all fine roots) in all varieties (e.g. Fig. 4D, E, I, J; see also Supplementary Fig. S4N, O, S, T at *JXB* online). The four varieties allocated between 80% (Endurance) and 90% (Resolution) of the dry matter to the AGB. Stem and stool biomass data at the end of rotations showed that all varieties allocated a smaller fraction of assimilates to BGB during R2

compared with R1. For Endurance, this dropped from 20 to 15%, while Tora reduced allocation from 15.4 to 11.3%.

Model validation

Validation using the variety trial at ROTH

The model validation was first done by comparing the average LAI, stem height and number, and AGB/BGB yields measured in the second rotation of growth (R2) at the dedicated variety trial at ROTH with the corresponding simulations (Table 3). The model predicted the differences in LAI between varieties well, with values for Endurance being highest and for Tora the lowest (Fig. 4). However, LAI modelling efficiency was low due to a phase shift of regrowth during the first year of the second rotation. Separating coppicing from non-coppicing years improved the statistical indicators of the prediction of LAI data (RMSE=0.76; MD=-0.23; $R^2=0.61$).

Table 3. Goodness of fit for modelling growth indicators

LAI, canopy height (h_c), number of stems (n_{stems}), biomass of stem (B_{stem}) and stool (B_{stool}), and overall yield of the four willow varieties grown at ROTH for the first (R1, 2010–2011) and second (R2, 2012–2013) rotation were used for validation. RMSE, residual mean square error; MD, mean difference; ME, modelling efficiency; R^2 , certainty.

Variety	Indicator	RMSE		MD (O–S)		ME		R ²	
		R1	R2	R1	R2	R1	R2	R1	R2
Endurance	LAI (m ² m ⁻²)	0.95	1.78	-0.09	-1.24	0.07	-0.45	0.25	0.38
	h_c (m)	0.30	0.26	-0.18	-0.08	0.89	0.96	0.95	0.97
	n_{stems} (m ⁻²)	6.39	7.24	4.40	2.97	0.02	0.15	0.55	0.95
	B_{stem} (Mg ha ⁻¹)	1.98	0.87	1.49	0.39	0.90	0.99	0.96	1.00
	B_{stool} (Mg ha ⁻¹)	1.37	2.38	0.85	1.74	-0.03	-0.06	0.62	0.58
Resolution	LAI (m ² m ⁻²)	0.70	0.93	0.45	-0.40	-2.67	-0.23	0.03	0.37
	h_c (m)	0.29	0.32	0.16	-0.18	0.94	0.94	0.96	0.96
	n_{stems} (m ⁻²)	6.64	4.04	3.92	2.04	-0.18	-0.15	0.78	0.66
	B_{stem} (Mg ha ⁻¹)	1.86	1.20	0.39	-0.91	0.89	0.99	0.90	1.00
	B_{stool} (Mg ha ⁻¹)	0.80	1.57	0.53	1.19	-0.10	-0.01	0.84	0.95
Terra Nova	LAI (m ² m ⁻²)	0.79	1.17	0.35	-0.63	-0.96	-1.07	0.03	0.35
	h_c (m)	0.23	0.31	0.14	0.16	0.94	0.93	0.96	0.96
	n_{stems} (m ⁻²)	3.87	2.58	-0.19	1.18	0.30	0.11	0.74	0.46
	B_{stem} (Mg ha ⁻¹)	1.73	0.99	-0.36	0.22	0.91	0.99	0.95	0.99
	B_{stool} (Mg ha ⁻¹)	1.02	1.30	-0.74	-1.29	-0.02	-0.06	0.94	1.00
Tora	LAI (m ² m ⁻²)	0.45	1.17	0.10	-0.61	-0.63	-1.54	0.15	0.28
	h_c (m)	0.16	0.21	-0.03	0.03	0.97	0.98	0.98	0.98
	n_{stems} (m ⁻²)	2.28	5.15	0.43	4.21	0.44	-1.45	0.76	0.76
	B_{stem} (Mg ha ⁻¹)	1.69	0.11	0.04	0.11	0.85	1.00	0.95	1.00
	B_{stool} (Mg ha ⁻¹)	0.64	0.96	-0.52	0.49	-0.33	0.56	0.91	0.91
All*	B_{stem} (Mg ha ⁻¹)	1.81	0.89	0.38	-0.05	0.90	0.99	0.92	0.99
	B_{stool} (Mg ha ⁻¹)	1.00	1.64	0.06	0.53	0.22	0.28	0.26	0.41

*Due to a small number of observations during R2 for biomass ($n=3$ compared with >10 for the other indicators), the data were pooled together to give an overall estimation.

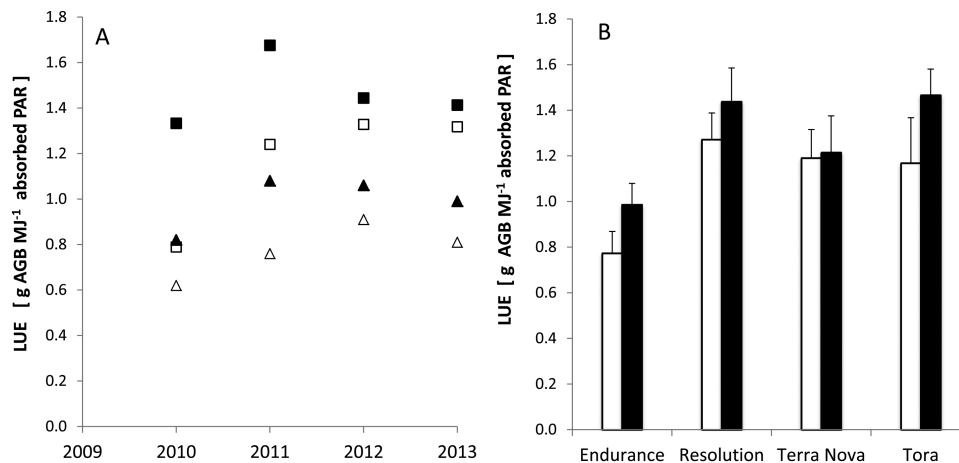


Fig 5. Simulated average light use efficiency (LUE, g AGB MJ⁻¹ APAR) during the time course of the experiment (2010–2013) for the varieties Tora (squares) and Endurance (triangles) at ROTH (open symbols) and ABER (closed symbols) (A) and averaged for all varieties at both sites (B). The error bars represent the standard deviation.

A management×site effect was observed in terms of different stem numbers and height/diameter ratio between ABER versus ROTH across all four varieties (Fig. 6). These observations suggested site-specific parameter values for AGB/BGB partitioning and initial stem numbers and height/thickness (m_{DH}).

The final yield predictions agreed in a satisfactory way with the empirical data at ROTH for all four willow varieties

for both rotations (R1, cross-validation, and R2, validation) (Fig. 7). This result was consistent with the fact that for all varieties we observed a high ME and R^2 (>0.85 , Table 3) for stem biomass. The daily simulations for LAI, stem height, and biomass, as well as stem number, were within the 95% confidence interval of mean observations of these variables (Fig. 4). The model was able to catch the behaviour of the

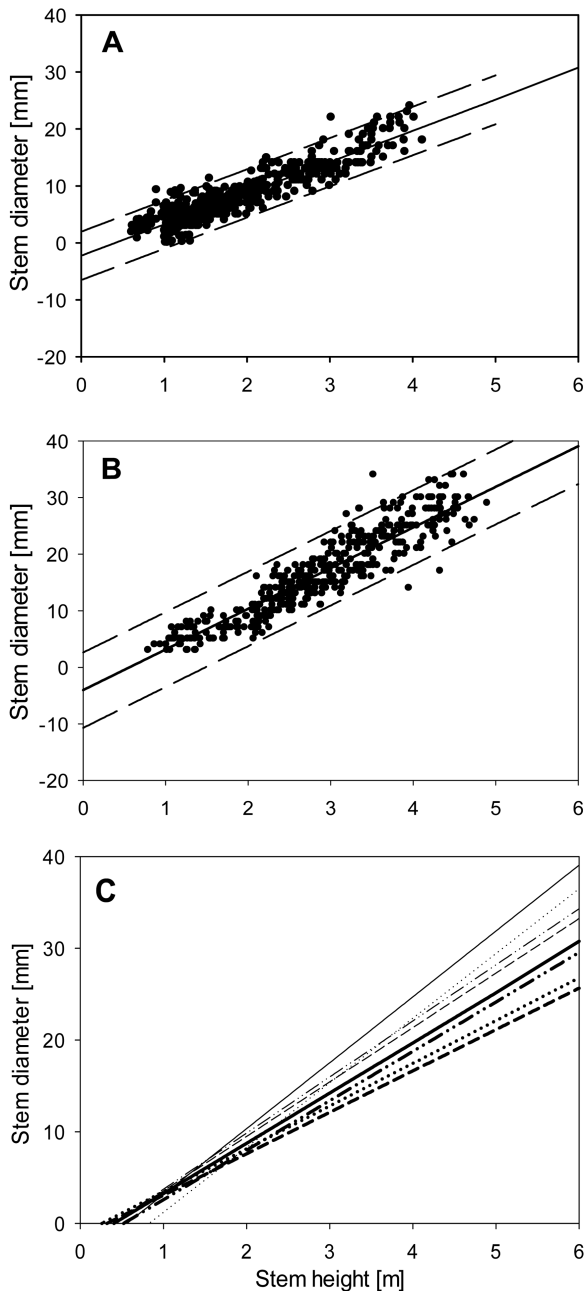


Fig. 6. Correlations between stem diameter and stem height for Endurance at ROTH (A) and ABER (B), and sketched for all willow varieties (Endurance —, Resolution - - -, Terra Nova ----, Tora for ROTH (bold lines) and ABER (fine lines) (C).

studied traits throughout the growing seasons for all studied willow varieties. The comparison between measured and simulated BGB was satisfactory for most varieties (Fig. 4E, J). ME was high for canopy height (all >0.9) and stem biomass yield (overall due to small number of samples ~0.99), and acceptable for BGB (overall ~0.28), while it was low for LAI and stem number (Table 3), due to slight asynchronies (Fig. 4).

It is interesting to observe that in wet years (2012; see Supplementary Table S2 at *JXB* online) broad-leaved varieties (e.g. Endurance, Fig. 4D) performed better than the others (e.g. Tora, Fig. 4I) but were more sensitive to WS in 2010. This is very clearly summarized in the yield calibration and validation (Fig.

7): in R1, low yields (7–11 Mg ha⁻¹ year⁻¹) reflected an overall establishment but also a drought (ROTH vs ABER) effect, mainly for broad-leaved varieties (END and TN, 29%). In comparison with R1 yields, R2 showed high yields at ROTH (12–14 Mg ha⁻¹ year⁻¹) with no drought effect, and establishment gains were larger for narrow- than for broad-leaved varieties (44 vs 24%). The narrow-leaved variety Resolution performed well in both rotations, irrespective of WS (see Supplementary Fig. S4 at *JXB* online), displaying an overall interesting G×E interaction. During the second rotation, final yields in all varieties were significantly lower at ABER than at ROTH. However, ABER second-rotation data could not be used for validation as the crop suffered exceptional wind damage that the model could not account for. Significant differences between genotypes ($P < 0.001$) established Endurance as the best yielding variety in both locations, in spite of its susceptibility to drought.

Validation with further yield data

Simulated and measured final biomass yields for the three varieties compared well at ROTH and LARS, irrespective of the length of the coppicing cycle (Fig. 8). The overall correlation between measured and simulated biomass yields across both locations was good ($R^2 = 0.80$) and the average difference was small and the ME high (MD = 0.68 Mg ha⁻¹; ME = 0.7). Most of the predictions were concentrated near the 1:1 line, proving that the model was able to reproduce actual yields. It showed a slight bias towards lower yields at LARS and overestimated yields at ROTH.

Discussion

The process-based model LUCASS characterized phenotypic carbon sinks and implemented a sink–source interaction to describe yield formation for different SRC willow genotypes. The novelty of this approach lies in its simplicity to parameterize the size of various sinks using phenotype-specific morphological characteristics. Calibrated and validated with data from sites across the UK, the model was able to illustrate the underlying system behaviour in terms of source and sink dynamics, and predicted final yields reflecting genotypic and environmental differences.

Key productivity parameters

Compared with other models (Deckmyn *et al.*, 2008; Amichev *et al.*, 2011; Tallis *et al.*, 2013), LUCASS has fewer parameters, and fewer than 20 proved to be crucial for yield formation (Fig. 2). The SA identified the onset of stem elongation, stem elongation rate, and diameter as key parameters for yield formation and indicators of vigour (Kauter *et al.*, 2003; Volk *et al.*, 2006). Parameters of early development, e.g. chilling and forcing functions (Cesaraccio *et al.*, 2004; Fu *et al.*, 2013), were confirmed to be important at sites with a mild winter climate (ABER and LARS). Despite the importance of the start of spring growth (Cannell and Smith, 1983; Weih, 2009), it is not entirely clear whether chilling has a physiological role (Horvath *et al.*, 2003; Rohde and Bhalerao, 2007) in addition to cold hardiness (Morin *et al.*, 2007). Ongoing investigations will elucidate whether chilling should be modelled for

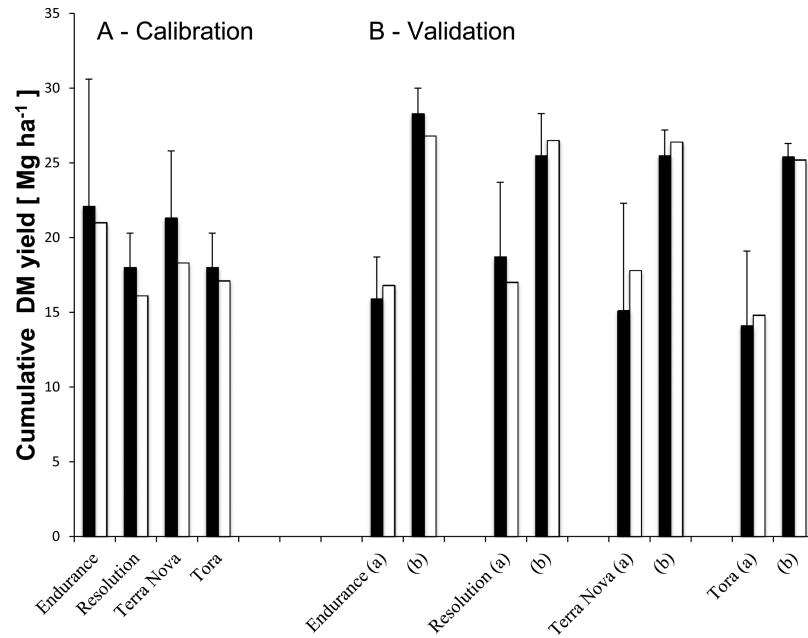


Fig. 7. Observed (filled columns) and simulated (open columns) accumulated yields of broad-leaved (Endurance, Terra Nova) and narrow-leaved (Resolution, Tora) willow varieties for calibration during the first coppice cycle (R1; 2010–2011) at ABER (a) and ROTH (b) (A) and validation over the second coppice cycle (R2; 2012–2013) at ROTH (B). DM, dry matter. The error bars represent the standard deviation of the observed yields.

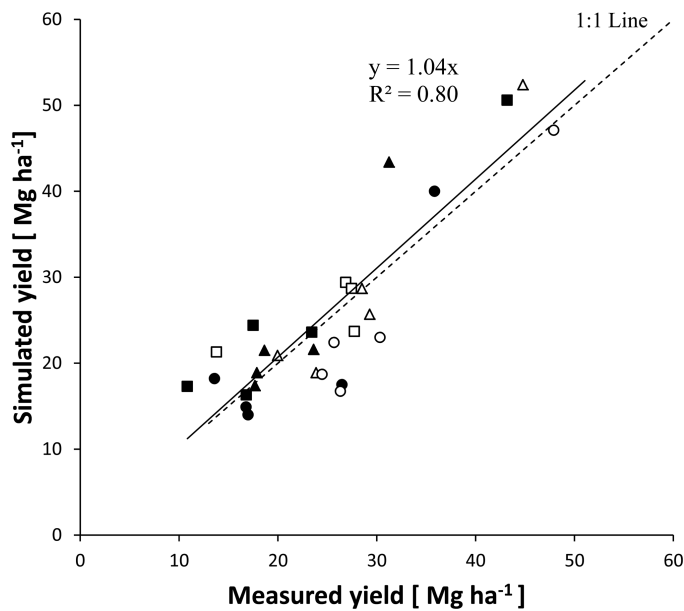


Fig. 8. Correlation between measured and simulated 2- and 3-year coppice biomass yields for the three willow varieties from trials at ROTH (closed symbols) and LARS (open symbols). Endurance, squares; Resolution, triangles; Tora, circles.

temperate tree species (Fu *et al.*, 2012). The role of photoperiod (Fu *et al.*, 2012) needs testing over a range of latitudes, as the sites studied here were similar. Nevertheless, this study did show that photoperiod was important for canopy development in terms of branching (dl_{BtoBr}) and stem elongation (dl_{OSER}).

This analysis also showed that early budburst does not necessarily mean faster canopy development. Despite initial delays after coppicing, e.g. 2012, modelled and observed LAIs reached their maxima at similar times and values, and

the disparity had no impact on biomass production. A late spring start was apparently compensated for by faster leaf growth when environmental conditions became favourable (Weih, 2009). Thus, although budburst date is important for modelling willow development (Savage and Cavender-Bares, 2011), it remains debatable whether its accuracy is also important for predicting yield (Tallis *et al.*, 2013).

Genotypic differences for routes to high yields?

Source formation

The variation of willow yield proved highly sensitive to parameters of LAI distribution and genotypic canopy characteristics, confirming that stem dynamics and biomass yield are strongly influenced by radiation distribution within the canopy (Ceulemans *et al.*, 1996; Bullard *et al.*, 2002a; Tharakan *et al.*, 2008; Cerasuolo *et al.*, 2013). Photosynthesis parameters (A_{max} , φ_{pot}) differed across genotypes (Bonneau, 2004; Andralojc *et al.*, 2014) and were also confirmed as an important source of yield variation (Figs 2 and 3). Quantum efficiency (φ_{pot}) consistently caused a larger model response than A_{max} ; however, both seemed to be strongly related, as found by Andralojc *et al.* (2014) and Kaipainen (2009). Genotype ranking, according to photosynthetic capacity at the plant level, was dominated by leaf area, but genotypes realized similar biomass with different strategies, either through high photosynthetic rate or large leaf area, confirming previous results (Andralojc *et al.*, 2014).

LUE is a key physiological indicator, usually expressed in terms of woody AGB per unit absorbed PAR, which ranged from 0.6 to 1.7 g m⁻² MJ⁻¹ (Fig. 5A). Mean LUE was significantly higher at ABER (Fig. 5B), indicating its interaction with drought and senescence (Savage *et al.*, 2009), canopy duration,

and leaf abscission (Weih, 2009), which can affect cumulative photosynthesis (Philippot, 1996). These site-specific differences due to WS varied between broad- and narrow-leaved varieties (Endurance and Tora, respectively). Tora evaded drought by means of a smaller leaf number (Cerasuolo *et al.*, 2013) and LAI (Fig. 4F). The lowest LUE values were calculated for regrowth after first coppicing (2010), which was aggravated by drought at ROTH, especially for Endurance with its large canopy (−41%). *In situ* measurements under a controlled water supply showed a similar drop in photosynthetic efficiency (−33 to −60%; (Bonneau, 2004)). The range of average LUE (0.77–1.47 g MJ^{−1}), which was significantly different between sites ($P < 0.01$) and varieties ($P < 0.001$), agreed with the range of simulated values (Jing *et al.*, 2012) and other estimates (Bullard *et al.*, 2002a; Sannervik *et al.*, 2006; Tallis *et al.*, 2013). A large canopy increased a variety's sensitivity to WS, e.g. the lowest LUE of Endurance irrespective of location, but achieved high yields in wet conditions. The effects of senescence on nutrient remobilization (Fracheboud *et al.*, 2009) and dry matter loss through respiration (de Neergaard *et al.*, 2002) can complicate the G×E interaction under variable climate conditions.

Sink formation

Morphological characteristics were the most important to identify high-yielding genotypes especially under WS conditions. The high sensitivity of these sink parameters across both sites (Figs 2 and 3) confirmed their importance for yield formation (Larsson, 1998). Traits such as stem number, height, and diameter, as well as leaf size and form, are also easily measured in high-throughput screenings (Sennerby-Forsse and Zsuffa, 1995; Bullard *et al.*, 2002b; Martin and Stephens, 2006; Sannervik *et al.*, 2006; Verwijst *et al.*, 2012).

Our results confirmed earlier findings that Endurance has the thickest stems while Resolution has the thinnest (Cunniff *et al.*, 2011). The genotype-specific relationship between stem diameter and height (Fig. 6) is an excellent example of integrating plant characteristics and environment influence (G×E interaction). Stem diameter increases with the length of the coppicing cycle and is an important determinant for harvestable wood volume (Bullard *et al.*, 2002b; Amichev *et al.*, 2011).

Moreover, parameter values for the potential allocated AGB were considered to be ~10–12% lower than those estimated from destructive measurements. This was due to the concurrence of two factors: around 30–40% of the net primary production produced by basket willow was used below ground, in particular on fine roots due to their high turnover rate (Rytter, 2001). Experimental evidence provided by soil cores collected at ROTH showed that actual fine-root biomass was up to three times that from destructive samples, e.g. Endurance 873 vs 283 g m^{−3}, respectively (Cunniff *et al.*, 2015). These root cores also showed that willows had a 65% greater fine-root volume when grown at ABER compared with growth at ROTH.

The analysis of the experiments showed differences in carbon storage in BGB (Cunniff *et al.*, 2015), which could have affected the regrowth dynamics (Sennerby-Forsse and Zsuffa, 1995; Tharakan *et al.*, 2008; Verwijst *et al.*, 2012). Poor yields of Tora under drought were shown to be concurrent with low initial BGB. Root biomass could be a key trait to mitigate

such circumstances (Ceulemans *et al.*, 1996). Tora showed great resilience to high yield in the second growth cycle by building up a comparable fine-root mass (Cunniff *et al.*, 2015). However, the G×E interaction was not conclusive: in spite of more investment of carbon in BGB at ABER, the vigour after coppicing in 2012 dropped considerably (Cunniff *et al.*, 2015). Experimental data also showed significant differences in biomass allocation among varieties ($P < 0.001$) and in the interaction between site and variety ($P < 0.05$) (Cunniff *et al.*, 2011, 2015). Stem numbers were possibly related to soluble sugars/starch availability, but were difficult to separate from management effects (cut-back) at ABER, which resulted in a smaller stool volume with fewer buds to develop into new stems (Cunniff *et al.*, 2014).

Further analyses of the underlying physiological processes are needed to justify different modelling approaches for early development (Fu *et al.*, 2012) and the impact on early growth (Tharakan *et al.*, 2008; Verwijst *et al.*, 2012) and yield formation. A systematic budburst delay after coppicing can be expected (Verwijst *et al.*, 2012). Bud and stem numbers could be influenced by stool size (management effect), as well as starch and sugar contents (Tschaplinski and Blake, 1995; Cunniff *et al.*, 2014). This and evidence in regard to regrowth after coppicing (Tschaplinski and Blake, 1994; Von Fircks and Sennerby-Forsse, 1998) suggest model expansion to describe the number of buds bursting as a function of readily available carbohydrate.

BGB characterization within the system is essential (Karp and Shield, 2008), but few data exist for roots of SRC (Rytter, 2001; Pacaldo *et al.*, 2013; Agostini *et al.*, 2015; Cunniff *et al.*, 2015). Destructive harvests represented only part of the below-ground allocation underestimating fine root biomass between 16 and 24% (Cunniff *et al.*, 2015). Biomass in the fine root mass in a 1 m profile ranged from 3.56 to 6.46 Mg ha^{−1} for Tora and Endurance, respectively (unpublished data), a fraction that is likely to turn over fast (Rytter, 2001).

Source–sink interactions under different environments

Within the sink–source interaction, LAI and stem growth play the key roles for potential production, balancing the available carbohydrate for resource capture and harvestable biomass. A hierarchy of dry matter allocation to leaves over stems was needed to enable sufficient light capture. In the model, LAI is influenced by budburst and base temperature for leaf growth, which usually precede the day length threshold for stem elongation. Sufficient allocation of carbohydrate to leaves (and fine roots) was secured by considering a genotype-specific base temperature for stem elongation, T_{bStE} , in the range of 8–10 °C independent of location. These experimentally founded values are much higher than those suggested for the variety Jorr (2–7.6 °C) (Martin and Stephens, 2008). The discrepancy between these base temperatures for shoot extension is probably due to a different interpretation of this parameter. In contrast to base temperature within a linear function of stem elongation rate and air temperature (Martin and Stephens, 2008), LUCASS used T_{bStE} to switch carbon allocation from ‘leaves only’ (T_B) to ‘leaves+stems’, with stem elongation mainly depending on day length.

LAI values between 2 and 4 were sufficient to reach a high biomass yield (Jing *et al.*, 2012), suggesting that, with the exception of Endurance, all varieties were source limited during the first year of regrowth (Fig. 4 and Supplementary Fig. S3 at *JXB* online). As LUCASS simulated the seasonal dynamics of carbohydrate reserves explicitly, the reserve pools balanced the seasonal fluctuations in carbon availability. Overall, the agreement between measured and modelled sink indicators was good across the validation datasets (Table 3), even for stem numbers, although the dynamic of stem numbers was less well represented (Fig. 4). According to our simulations, the stem as the major sink accounted for 75–97% of the yield variance, variation of stool weights (Fig. 4; 47–95%), and plausible values for root dry matter. Furthermore, 94 and 80% of the yield variance was captured across cross-validation at ROTH and independent data sets (LARS and ROTH), respectively.

The necessity to define site-specific initial bud and stem numbers to compensate for environmental and management (coppicing) effects shows the need for a more mechanistic description of the coppicing response. Stored carbohydrates in the reserve pools are essential for the initial growth of perennials (Philippot, 1996), and the available evidence (Cunniff *et al.*, 2014, 2015) would allow implementation of a functional relationship between reserve availability and stem/bud numbers to describe regrowth (Bullard *et al.*, 2002b; Tharakan *et al.*, 2008).

Allocation to BGB was a limiting factor for development of AGB during crop establishment and can be considered as one cause for low yield during the first rotation. Water limitation caused a further significant reduction of AGB in favour of BGB at ROTH, and LUCASS simulated both limitations adequately. The varieties showed different responses towards WS from a very sensitive Endurance to an almost tolerant Resolution (Bonneau, 2004; Savage and Cavender-Bares, 2011; Larsen *et al.*, 2014). New evidence from specific experiments with potential- and limited-water treatments will follow in future.

From this analysis we suggest that the LUCASS model can be used first to accelerate the selection and optimization of genotypes in breeding programmes, and secondly to predict the site-specific yields of different SRC willow genotypes. Although details of the budburst modelling are still in progress, the current model can also be used to explore climate and management scenarios for the production of biomass resources in the bioeconomy. The ability of LUCASS to simulate allocation to BGB (stool, and coarse and fine roots) also helps to quantify the ecosystem functions of regrowth, soil-specific resource capture, and the carbon balance. Ongoing work will also provide more details on the sustainability of canopy and rooting phenotypes in different hydrological and agrometeorological situations.

Supplementary data

Supplementary data are available at *JXB* online.

Model equations S1–S7.

Fig. S1. Canopy (1) and leaf (2) phenotypes for open, narrow-leaved Tora (A) and closed, broad-leaved Endurance (B).

Fig. S2. Global solar radiation (---), air temperature (—) and precipitation (filled bar) at Rothamsted (A) and Aberystwyth (B) during the experiment (2010–13).

Fig. S3. Heat map from sensitivity analysis displaying the average response strength (μ) estimated using the Morris method, run for all varieties at both sites, Harpenden (ROTH) and Aberystwyth (ABER) with weather data for first (R1, 2010–11) and second rotation (R2, 2012–13).

Fig. S4. Observed (filled symbols) and simulated (solid line) leaf area index (LAI), canopy height, stem number and accumulated stem (AGB) and stool (BGB) biomass of Resolution (K–O) and Terra Nova (P–T) grown at Rothamsted over two consecutive 2-year rotations (2010–2011; 2012–2013).

Table S1. Physical characteristics of the soil in three sites using the Soil Classification System for England and Wales: Harpenden (ROTH), Aberystwyth (ABER) and Long Ashton Research Station (LARS).

Table S2. Cumulative annual precipitation, radiation, and average minimum and maximum temperature (2010–2013) at the two sites (ROTH and ABER).

Table S3. Optimized values of the parameters T_C and C_r of the chilling model for each willow variety.

Table S4. Results of the sensitivity analysis for ROTH and ABER simulated under potential (NWS) and water-limited (WS) production for (a) the first (2010–2011) and (b) the second (2012–2013) coppice rotation.

Table S5. Parameter values for the stem height/diameter relationship for the four studied varieties (Endurance, Resolution, Terra Nova, and Tora) and the two dedicated trials (ROTH and ABER).

Acknowledgements

The authors would like to thank the Biotechnological and Biological Sciences Research Council (BBSRC) and Ceres Inc. for funding this work within the ‘BBSRC Sustainable Bioenergy Centre (BSBEC): Perennial Bioenergy Crops Programme’ (BB/G016216/1; <http://www.bsbec-biomass.org.uk/>). We also acknowledge funding through the Institute Strategic Program Grant ‘Cropping Carbon’. We would also like to thank Tim Barraclough, March Castle, William Macalpine, and Peter Fruen (Rothamsted), and Anne Maddison and Laurence Jones (Aberystwyth) for their dedicated work collecting data in the field.

References

- Agostini F, Gregory AS, Richter GM. 2015. Carbon sequestration by perennial energy crops: is the jury still out? *BioEnergy Research* **8**, 1057–1080.
- Amichev BY, Hanks RD, Van Rees KCJ. 2011. A novel approach to simulate growth of multi-stem willow in bioenergy production systems with a simple process-based model (3PG). *Biomass and Bioenergy* **35**, 473–488.
- Andralojc PJ, Bencze S, Madgwick PJ, Philippe H, Powers SJ, Shield I, Karp A, Parry MAJ. 2014. Photosynthesis and growth in diverse willow genotypes. *Food and Energy Security* **3**, 69–85.
- Aylott MJ, Casella E, Tubby I, Street NR, Smith P, Taylor G. 2008. Yield and spatial supply of bioenergy poplar and willow short-rotation coppice in the UK. *New Phytologist* **178**, 358–370.
- Bonneau LJG. 2004. Drought resistance of willow short rotation coppice genotypes. PhD thesis, Cranfield University, Silsoe, UK.
- Bullard MJ, Mustill SJ, Carver P, Nixon PMI. 2002a. Yield improvements through modification of planting density and harvest

- frequency in short rotation coppice *Salix* spp.—2. Resource capture and used in two morphologically diverse varieties. *Biomass & Bioenergy* **22**, 27–39.
- Bullard MJ, Mustill SJ, McMillan SD, Nixon PMI, Carver P, Britt CP.** 2002b. Yield improvements through modification of planting density and harvest frequency in short rotation coppice *Salix* spp.—1. Yield response in two morphologically diverse varieties. *Biomass & Bioenergy* **22**, 15–25.
- Cannell MGR, Smith RI.** 1983. Thermal time, chill days and prediction of budburst in *Picea sitchensis*. *Journal of Applied Ecology* **20**, 951–963.
- Cerasuolo M, Richter GM, Cunniff J, Purdy S, Shield I, Karp A.** 2013. A pseudo-3D model to optimise the target traits of light interception in short-rotation coppice willow. *Agricultural and Forest Meteorology* **173**, 127–138.
- Cesaraccio C, Spano D, Snyder RL, Duce P.** 2004. Chilling and forcing model to predict bud-burst of crop and forest species. *Agricultural and Forest Meteorology* **126**, 1–13.
- Ceulemans R, McDonald AJ, Pereira JS.** 1996. A comparison among eucalypt, poplar and willow characteristics with particular reference to a coppice, growth-modelling approach. *Biomass & Bioenergy* **11**, 215–231.
- Chaine I.** 2000. A unified model for budburst of trees. *Journal of Theoretical Biology* **207**, 337–347.
- Cunniff J, Purdy SJ, Barraclough T, Castle M, Maddison AL, Jones LE, Shield IF, Gregory AS, Karp A.** 2015. High yielding biomass ideotypes of willow (*Salix* spp.) show differences in below ground biomass allocation. *Biomass & Bioenergy* **80**, 114–127.
- Cunniff J, Shield I, Barraclough T, et al.** 2011. BSBE-CBioMASS—Selecting traits to optimise biomass yield of SRC willow. *Aspects of Applied Biology*, **112**, 83–91.
- Cunniff J, Shield I, Purdy S, Karp A.** 2014. Phenological dynamics of above and below ground biomass and non- structural carbohydrates in the perennial bioenergy crop willow. In: International Poplar Symposium, University of British Columbia in Vancouver, Canada.
- de Neergaard A, Porter JR, Gorissen A.** 2002. Distribution of assimilated carbon in plants and rhizosphere soil of basket willow (*Salix viminalis* L.). *Plant and Soil* **245**, 307–314.
- De Pury DGG, Farquhar GD.** 1997. Simple scaling of photosynthesis from leaves to canopies without the errors of big-leaf models. *Plant, Cell and Environment* **20**, 537–557.
- Deckmyn G, Laureysens I, Garcia J, Muys B, Ceulemans R.** 2004. Poplar growth and yield in short rotation coppice: model simulations using the process model SECRETS. *Biomass & Bioenergy* **26**, 221–227.
- Deckmyn G, Verbeeck H, de Beeck MO, Vansteenkiste D, Steppe K, Ceulemans R.** 2008. ANAFORE: A stand-scale process-based forest model that includes wood tissue development and labile carbon storage in trees. *Ecological Modelling* **215**, 345–368.
- Fourcaud T, Zhang X, Stokes A, Lambers H, Korner C.** 2008. Plant growth modelling and applications: The increasing importance of plant architecture in growth models. *Annals of Botany* **101**, 1053–1063.
- Fracheboud Y, Luquez V, Bjorken L, Sjodin A, Tuominen H, Jansson S.** 2009. The Control of Autumn Senescence in European Aspen. *Plant Physiology* **149**, 1982–1991.
- Fu YH, Campioli M, Deckmyn G, Janssens IA.** 2013. Sensitivity of leaf unfolding to experimental warming in three temperate tree species. *Agricultural and Forest Meteorology* **181**, 125–132.
- Fu YS, Campioli M, Van Oijen M, Deckmyn G, Janssens IA.** 2012. Bayesian comparison of six different temperature-based budburst models for four temperate tree species. *Ecological Modelling* **230**, 92–100.
- Genard M, Dazat J, Franck N, Lescourret F, Moitrier N, Vaast P, Vercambre G.** 2008. Carbon allocation in fruit trees: from theory to modelling. *Trees-Structure and Function* **22**, 269–282.
- Goudriaan J.** 1988. The Bare Bones of Leaf-Angle Distribution in Radiation Models for Canopy Photosynthesis and Energy Exchange. *Agricultural and Forest Meteorology* **43**, 155–169.
- Goudriaan J, van Laar HH.** 1994. Modelling Potential Crop Growth Processes. Textbook with Exercises. Wageningen: Kluwer Academic Publishers.
- Guidi W, Tozzini C, Bonari E.** 2009. Estimation of chemical traits in poplar short-rotation coppice at stand level. *Biomass & Bioenergy* **33**, 1703–1709.
- Heilman PE, Ekuan G, Fogle D.** 1994. Aboveground and belowground biomass and fine roots of 4-year-old hybrids of *Populus trichocarpa* × *Populus deltoides* and parental species in short-rotation culture. *Canadian Journal of Forest Research* **24**, 1186–1192.
- Hlaszny E, Hajdu E, Gy B, Ladanyi M.** 2012. Comparison of budburst models predictions for Kekfrankos. *Applied Ecology and Environmental Research* **10**, 75–86.
- Hoeglund M, Hanslin HM, Van Oijen M.** 2005. Timothy regrowth, tillering and leaf area dynamics following spring harvest at two growth stages. *Field Crops Research* **93**, 51–63.
- Horvath DP, Anderson JV, Chao WS, Foley ME.** 2003. Knowing when to grow: signals regulating bud dormancy. *Trends in Plant Science* **8**, 534–540.
- Jing Q, Conijn SJG, Jongschaap REE, Bindraban PS.** 2012. Modeling the productivity of energy crops in different agro-ecological environments. *Biomass and Bioenergy* **46**, 618–633.
- Kaipainen E.** 2009. Parameters of photosynthesis light curve in *Salix dasycladus* and their changes during the growth season. *Russian Journal of Plant Physiology* **56**, 445–453.
- Karp A, Hanley SJ, Trybush SO, Macalpine W, Pei M, Shield I.** 2011. Genetic improvement of willow for bioenergy and biofuels. *Journal of Integrative Plant Biology* **53**, 151–165.
- Karp A, Richter GM, Shield IF, Hanley SH.** 2014. Genetics, genomics and crop modelling: integrative approaches to the improvement of biomass willows. In: McCann MC, Buckeridge MS, Carpita NC, eds. *Plants and bioenergy*, Vol. 4. New York: Springer Science+Business Media, 107–130.
- Karp A, Shield I.** 2008. Bioenergy from plants and the sustainable yield challenge. *New Phytologist* **179**, 15–32.
- Kauter D, Lewandowski I, Claupein W.** 2003. Quantity and quality of harvestable biomass from *Populus* short rotation coppice for solid fuel use—a review of the physiological basis and management influences. *Biomass and Bioenergy* **24**, 411–427.
- Larsen S, Jørgensen U, Lærke P.** 2014. Willow yield is highly dependent on clone and site. *BioEnergy Research* **7**, 1280–1292.
- Larsson S.** 1998. Genetic improvement of willow for short-rotation coppice. *Biomass and Bioenergy* **15**, 23–26.
- Laureysens I, Deraedt W, Indeherberge T, Ceulemans R.** 2003. Population dynamics in a 6-year old coppice culture of poplar. I. Clonal differences in stool mortality, shoot dynamics and shoot diameter distribution in relation to biomass production. *Biomass and Bioenergy* **24**, 81–95.
- Le Roux X, Lacoine A, Escobar-Gutierrez A, Le Dizes S.** 2001. Carbon-based models of individual tree growth: a critical appraisal. *Annals of Forest Science* **58**, 469–506.
- Martin PJ, Stephens W.** 2006. Willow growth in response to nutrients and moisture on a clay landfill cap soil. I. Growth and biomass production. *Bioresource Technology* **97**, 437–448.
- Martin PJ, Stephens W.** 2008. Willow water uptake and shoot extension growth in response to nutrient and moisture on a clay landfill cap soil. *Bioresource Technology* **99**, 5839–5850.
- Matthews RW.** 2001. Modelling of energy and carbon budgets of wood fuel coppice systems. *Biomass and Bioenergy* **21**, 1–19.
- McDonald AJ, Stadenberg I.** 1993. Diurnal pattern of leaf extension in *Salix viminalis* relates to the difference in leaf turgor before and after stress relaxation. *Tree Physiology* **13**, 311–318.
- Morin X, Ameglio T, Ahas R, Kurz-Besson C, Lanta V, Lebourgeois F, Miglietta F, Chuine I.** 2007. Variation in cold hardiness and carbohydrate concentration from dormancy induction to bud burst among provenances of three European oak species. *Tree Physiology* **27**, 817–825.
- Morris MD.** 1991. Factorial sampling plans for preliminary computational experiments. *Technometrics* **33**, 161–174.
- Pacaldo RS, Volk TA, Briggs RD.** 2013. Greenhouse gas potentials of shrub willow biomass crops based on below- and aboveground biomass inventory along a 19-year chronosequence. *BioEnergy Research* **6**, 252–262.
- Payne RW, Harding SA, Murray DA, Soutar DM, Baird DB, Glaser AI, Welham SJ, Gilmour AR, Thompson R, Webster R.** 2011. *The Guide to Genstat release 14*. Hemel Hempstead, UK: VSN International.

- Penning de Vries FWT, Van Laar HH, Chardon MCM.** 1983. Bioenergetics of growth of seeds, fruits and storage organs. In: Smith WH, Banta SJ, eds. Potential productivity of field crops under different environments. Los Banos, The Philippines: IRRI, 37–59.
- Perttu KL, Philippot S.** 1996. Modelling short rotation forestry growth (Uppsala, Sweden, 24–26 October 1994). *Biomass and Bioenergy* **11**, 69–71.
- Philippot S.** 1996. Simulation models of short-rotation forestry production and coppice biology. *Biomass and Bioenergy* **11**, 85–93.
- Porter JR, Parfitt RI, Arnold GM.** 1993. Leaf demography in willow short-rotation coppice. *Biomass and Bioenergy* **5**, 325–336.
- Powers SJ, Peacock L, Yap ML, Brain P.** 2006. Simulated beetle defoliation on willow genotypes in mixture and monotype plantations. *Annals of Applied Biology* **148**, 27–38.
- Pretzsch H, Grote R, Reineking B, Roetzer T, Seifert S.** 2008. Models for forest ecosystem management: a European perspective. *Annals of Botany* **101**, 1065–1087.
- Richter GM, Acutis M, Trevisiol P, Latiri K, Confalonieri R.** 2010. Sensitivity analysis for a complex crop model applied to Durum wheat in the Mediterranean. *European Journal of Agronomy* **32**, 127–136.
- Richter GM, Rana G, Ferrara RM, et al.** 2006. Stability and mitigation of arable systems in hilly landscapes. Brussels: European Commission, 280.
- Rinne PLH, Welling A, Vahala J, Ripel L, Ruonala R, Kangasjarvi J, van der Schoot C.** 2011. Chilling of dormant buds hyperinduces FLOWERING LOCUS T and recruits GA-inducible 1,3- β -glucanases to reopen signal conduits and release dormancy in *Populus*. *The Plant Cell* **23**, 130–146.
- Robinson KM, Karp A, Taylor G.** 2004. Defining leaf traits linked to yield in short-rotation coppice *Salix*. *Biomass and Bioenergy* **26**, 417–431.
- Rohde A, Bhalerao RP.** 2007. Plant dormancy in the perennial context. *Trends in Plant Science* **12**, 217–223.
- Rytter RM.** 2001. Biomass production and allocation, including fine-root turnover, and annual N uptake in lysimeter-grown basket willows. *Forest Ecology and Management* **140**, 177–192.
- Sampson DA, Ceulemans R.** 2000. SECRETS: simulated carbon fluxes from a mixed coniferous/deciduous Belgian forest. In: Ceulemans R, Veroustraete F, Gond V, Van Rensbergen JBHF, eds. Forest ecosystem modeling, upscaling and remote sensing. The Netherlands: SPB Academic Publishing, 95–108.
- Sannervik AN, Eckersten H, Verwijst T, Kowalik P, Nordh N-E.** 2006. Simulation of willow productivity based on radiation use efficiency, shoot mortality and shoot age. *European Journal of Agronomy* **24**, 156–164.
- Savage JA, Cavender-Bares J, Verhoeven A.** 2009. Willow species (genus: *Salix*) with contrasting habitat affinities differ in their photoprotective responses to water stress. *Functional Plant Biology* **36**, 300–309.
- Savage JA, Cavender-Bares JM.** 2011. Contrasting drought survival strategies of sympatric willows (genus: *Salix*): consequences for coexistence and habitat specialization. *Tree Physiology* **31**, 604–614.
- Schapendonk AHCM, Stol W, van Kraalingen DWG, Bouman BAM.** 1998. LINGRA, a sink/source model to simulate grassland productivity in Europe. *European Journal of Agronomy* **9**, 87–100.
- Sennerby-Forsse L, Zsuffa L.** 1995. Bud structure and resprouting in coppiced stools of *Salix viminalis* L., *S. eriocephala* Michx., and *S. amygdaloides* Anders. *Trees—Structure and Function* **9**, 224–234.
- Sinclair TR.** 1986. Water and nitrogen limitations in soybean grain production. Part I. Model development. *Field Crops Research* **15**, 125–141.
- Smith P, Smith JU, Powelson DS, et al.** 1997. A comparison of the performance of nine soil organic matter models using datasets from seven long-term experiments. *Geoderma* **81**, 153–225.
- Stanton BJ, Serapiglia MJ, Smart LB.** 2014. The domestication and conservation of *Populus* and *Salix* genetic resources. In: Isebrands JG, Richardson J, eds. *Poplars and willows: trees for society and the environment*. Wallingford, UK: CAB International, 124–199.
- Tallis MJ, Casella E, Henshall PA, Aylott MJ, Randle TJ, Morison JLL, Taylor G.** 2013. Development and evaluation of ForestGrowth-SRC a process-based model for short rotation coppice yield and spatial supply reveals poplar uses water more efficiently than willow. *Global Change Biology Bioenergy* **5**, 53–66.
- Teixeira EI, Moot DJ, Brown HE, Pollock KM.** 2007. How does defoliation management impact on yield, canopy forming processes and light interception of lucerne (*Medicago sativa* L.) crops? *European Journal of Agronomy* **27**, 154–164.
- Tharakan PJ, Volk TA, Nowak CA, Ofezu GJ.** 2008. Assessment of canopy structure, light interception, and light-use efficiency of first year regrowth of shrub willow (*Salix* sp.). *BioEnergy Research* **1**, 229–238.
- Toillon J, Rollin B, Dalle E, Feinard-Duranceau M, Bastien J-C, Brignolas F, Marron N.** 2013. Variability and plasticity of productivity, water-use efficiency, and nitrogen exportation rate in *Salix* short rotation coppice. *Biomass and Bioenergy* **56**, 392–404.
- Tschaplinski TJ, Blake TJ.** 1994. Carbohydrate mobilization following shoot defoliation and decapitation in hybrid poplar. *Tree Physiology* **14**, 141–151.
- Tschaplinski TJ, Blake TJ.** 1995. Growth and carbohydrate status of coppice shoots of hybrid poplar following shoot pruning. *Tree Physiology* **15**, 333–338.
- van Laar HH, Goudriaan J, van Keulen H.** 1992. Simulation of crop growth for potential and water limited production situations (as applied to spring wheat). In: Simulation reports CABO-TT no. 27. Wageningen, The Netherlands: CABO-DLO/Theoretical Production Ecology, Wageningen Agricultural University.
- Verlinden MS, Broeckx LS, Van den Bulcke J, Van Acker J, Ceulemans R.** 2013. Comparative study of biomass determinants of 12 poplar (*Populus*) genotypes in a high-density short-rotation culture. *Forest Ecology and Management* **307**, 101–111.
- Verwijst T, Lundkvist A, Edelfeldt S, Forkman J, Nordh N-E.** 2012. Effects of clone and cutting traits on shoot emergence and early growth of willow. *Biomass and Bioenergy* **37**, 257–264.
- Vivin PH, Castelan M, Gaudillère JP.** 2002. A source/sink model to simulate seasonal allocation of carbon in grapevine. *Acta Horticulturae* **584**, 43–56.
- Volk TA, Abrahamson LP, Nowak CA, Smart LB, Tharakan PJ, White EH.** 2006. The development of short-rotation willow in the northeastern United States for bioenergy and bioproducts, agroforestry and phytoremediation. *Biomass and Bioenergy* **30**, 715–727.
- Von Fircks Y, Sennerby-Forsse L.** 1998. Seasonal fluctuations of starch in root and stem tissues of coppiced *Salix viminalis* plants grown under two nitrogen regimes. *Tree Physiology* **18**, 243–249.
- Weih M.** 2009. Genetic and environmental variation in spring and autumn phenology of biomass willows (*Salix* spp.): effects on shoot growth and nitrogen economy. *Tree Physiology* **29**, 1479–1490.
- Weih M, Nordh NE.** 2002. Characterising willows for biomass and phytoremediation: growth, nitrogen and water use of 14 willow clones under different irrigation and fertilisation regimes. *Biomass and Bioenergy* **23**, 397–413.
- Weih M, Nordh NE.** 2005. Determinants of biomass production in hybrid willows and prediction of field performance from pot studies. *Tree Physiology* **25**, 1197–1206.
- Wösten JHM, Lilly A, Nemes A, Le Bas C.** 1999. Development and use of a database of hydraulic properties of European soils. *Geoderma* **90**, 169–185.
- Xu X, Peng GQ, Wu CC, Korpelainen H, Li CY.** 2008. Drought inhibits photosynthetic capacity more in females than in males of *Populus cathayana*. *Tree Physiology* **28**, 1751–1759.